Manuscript of the paper entitled 'Changing directions of the tectonic structures, consistent paleomagnetic directions at the NE imbricated margin of Stable Adria' published in Tectonophysics 843 (2022).
Citation:
Márton, E., Ćosović, V., Imre, G., Velki, M. 2022: Changing directions of the tectonic structures, consistent paleomagnetic directions at the NE imbricated margin of Stable Adria. Tectonophysics 843, 229594.
https://doi.org/10.1016/j.tecto.2022.229594

Changing directions of the tectonic structures, consistent paleomagnetic directions at the NE imbricated margin of Stable Adria

Emő Márton [1], Vlasta Ćosović [2], Gábor Imre [1], Máté Velki [3, 1]

[1] Paleomagnetic Laboratory, Department of Geophysical Research, Szabályozott Tevékenységek Felügyeleti Hatósága. Columbus 17-23, 1145 Budapest, Hungary

[2] Department of Geology, Faculty of Science, University of Zagreb, Horvatovac 102b, 10000 Zagreb, Croatia

[3] Department of Geophysics and Space Science, Eötvös Loránd University. Pázmány Péter 1/C, 1117 Budapest, Hungary

Abstract

The imbricated margin of stable Adria, which belongs to the External Dinarides, comprises a chain of islands, which follow the dominant NW-SE Dinaric trend in the northern segment, while the dominant tectonic orientation changes to WNW-ESE in the central Adriatic area, near Split. The new paleomagnetic results documented in this paper are from the islands of the latter and can be interpreted in terms of tectonics together with already published robust data sets from the Northern Adriatic Islands and stable Adria, respectively. The problems addressed are the proposed extra CCW rotation in the central Adriatic area relative to the rest of the Dinarides, the differences in the tectonostratigraphic models of the offshore External Dinarides, the relationship to Stable Adria and the reason for the arcuated shape of the thrust front between stable and imbricated Adria.

From the five largest Central and Southern Adriatic Islands over 1000 independently oriented cores, representing 98 Upper Tithonian – Paleocene carbonate localities, were subjected to standard laboratory processing of the natural remanent magnetization, component analysis, and statistical evaluation on locality and between locality levels. The results lead to the conclusion that these islands moved in close co-ordination with both, the Northern Adriatic Islands and stable Adria, at least from the Albian on. The different tectonic trends characterizing the islands and reflected also in the arcuated shape of the thrust front between Stable and Imbricated Adria is explained by the dominance of one of the Late Cretaceous and younger compressional strain fields. The structures due to the Late Cretaceous strain field are dominant in Cres island (N-S trend), the ones formed during the Late Eocene-Early Oligocene prevail in the Northern Adriatic islands (NW-SE trend), SE of Cres. The WSW-ENE general orientation of the structures in the Central Adriatic area is due to the strong neotectonic deformation.

Key words

Offshore External Dinarides, shallow water carbonates, updated biostratigraphy, paleomagnetism, tectonic structures

Highlights

There is no evidence for post-Aptian relative movement between the Adriatic islands

The changing tectonic trend of the islands reflect differently oriented strain fields

The Adriatic islands moved in close co-ordination with stable Adria after the Aptian

The arcuated thrust front SW of the islands matches the tectonic trend of the islands

Introduction

The NE imbricated margin of stable Adria is considered as belonging to the Dinarides, which is a tectonically complex area between stable Adria in the SW and Europe in the NE. The tectonic evolution and the paleogeography of the Dinarides have been the subject of numerous studies, reviewed e.g. by Dimitrijević (1982) and with the incorporation of subsequent observations and data, interpreted in terms of plate tectonics e.g. by Herak (1986), Pamić et al. (1998), Tari (2002), Schmid et al. (2008), Korbar (2009). The Dinarides comprise the Inner and the Outer or External Dinarides. The boundary between them is defined differently by different authors (e.g., Pamić et al., 1998, Tari, 2002, Vlahović et al., 2005 Tomljenović et al., 2008). The External Dinarides are further subdivided into units which are, in their turn, differently named and interpreted from tectonostratigraphic point of view. There seems to be, however, a general agreement about an important tectonic boundary within the External Dinarides, which is a complex system of fold and thrusts named North – Eastern Adriatic Trough by Korbar (2009), running in NW-SE direction, following the Adriatic coastline (Grandić et al., 2013). The Adriatic islands belong to a belt situated SW from this thrust front and are subdivided into a northern, a central and a southern segment.

The northern segment is characterized by a general N-S, the central segment by NW-SE trend and the southern segment by E-W tectonic trend (Fig. 1). Vertical axis counterclockwise (CCW) rotation was offered to explain the deviation of the latter from the general Dinaridic tectonic trend (Aljinović et al., 1987). However, Marinčić (1997) strongly opposed such model. When studying the tectonic structures on the island of Hvar in detail he came to the conclusion that deformations related to the Dinaridic orogen in the Late Cretaceous (known as Laramian phase) and Late Eocene (Pyrenean phase) andneotectonic activities (Miocene to recent times) resulted in the formation of folds with differently oriented axes (N-S, NW-SE and E-W respectively). In subsequent years, a number of papers published about Adriatic offshore dealt with the complexity of the deformation affecting the Adriatic islands (e.g., Prtoljan et al., 2007, Grandić et al., 2013, Saftić et al., 2019, Kastelic and Carafa, 2012). Although they expressed different views, they agreed that the structures in the External Dinarides formed through multiple stages of active compression.

As a results of systematic paleomagnetic studies from stable Adria and from the Northern Adriatic islands (Márton and Moro, 2009, Márton et al., 2008, 2010, 2011, 2014,

2017) a substantial data base allows us now to address the problem of the different tectonic trends in the Adriatic islands and their relationship to stable Adria, as the paleomagnetic method has the power to confirm or exclude the possibility of relative rotations. In order to facilitate direct comparison between the different segments of the archipelago, we shall present and document new result from Brač, Hvar, Korčula and Mljet islands and include earlier published data from Brač ((Márton et al., 2003, with updated stratigraphic ages) and Vis (Márton et al., 2014) islands.

The total number of studied localities from the Central and Southern Adriatic islands amounts to 98 of which 65 yielded good paleomagnetic directions. This is a relatively high proportion regarding the weak NRM intensities, characteristic of the shallow-water limestones of the Adriatic Carbonate Platform (e.g., Márton et al., 2008, 2014). The "reference" frame for checking the possible vertical axis CCW rotation of the Central and Southern Adriatic islands relative to stable Adria (Fig. 1, Adige embayment and stable Istria) and the Northern Adriatic islands (Fig. 1, Cres, Ist and surroundings islets, Dugi otok), respectively, is provided by published paleomagnetic results (Márton and Moro, 2009, Márton et al., 2008, 2010, 2011, 2014, 2017).

Geological settings

The Dinarides, stretching from the Southern Alps to the Albanides/Hellenides became a part of the Alpine orogenic system by the closure of (Neo)Tethys Ocean realm and associated basins from late Jurassic to Quaternary. The Dinarides are subdivided in two main tectonostratigraphic units, the External and the Internal Dinarides (e.g. Vlahović et al., 2005). The first is mainly built of Mesozoic shallow-water carbonate succession with subordinate occurrences of pelagic sediments, the second is ophiolite bearing with a complex succession of deep-water origin.

The Central Adriatic area, comprising the Central and Southern Adriatic islands, belongs to the External Dinarides, the site of very complex Mesozoic and Cenozoic geodynamic evolution (e.g. Pamić et al., 1998, Tari, 2002, Schmid et al., 2008, 2020, Korbar, 2009) recorded within a several kilometres thick sedimentary succession (e.g. Vlahović et al., 2005) starting from the Triassic rifting phase to the latest stage of the Alpine orogeny. Paleogeographically, the Central Adriatic area is considered as a part of the Adriatic carbonate platform, characterized by the dominance of shallow-water carbonates of Jurassic

through Paleocene–Eocene age. The platform sedimentation was punctuated by episodes of subaerial exposure or pelagic drowning. The most important events are the Early Aptian partial subsidence of the platform which correlates well with an anoxic oceanic event, Late Aptian-Early Albian sea-level fall, causing regional emersion which was followed by partial drowning of the platform until the end of the Santonian (Husinec and Jelaska, 2006, Prtoljan et al. 2007, Moro and Ćosović, 2013). The most prominent change in depositional regime took place during the Cretaceous-Paleogene sub-areal exposure recorded by regional unconformity, which was followed by flysch deposition during the Eocene–Oligocene foreland stage (Korbar, 2009; Ćosović et al., 2018).

The Central Adriatic area is characterized by limestones and in less portion, dolomites, of Upper Jurassic through Mid-Eocene age. Upper Jurassic sediments crop out on Mljet island only. Lower Cretaceous carbonates, sometimes strongly karstified and very often barren in fossils are known in Mljet, Korčula, Hvar and Vis islands. The Upper Cretaceous sediments, widespread on Brač, Hvar, Korčula and Vis islands, record facies differentiation (shallow-water and slope deposits). Paleogene sediments (ranging in age from K/Pg boundary to Middle to Late Eocene) with confined distribution, occur on Brač and Hvar islands.

The great portion of the island of Brač is made of carbonate deposits of Cenomanian through Maastrichtian age (Fig. 2). The Upper Cretaceous rock complex, up to 1500 m thick, is subdivided into six lithostratigraphic units based on benthic foraminifera and rudists remains (Gušić and Jelaska, 1990). Turonian deposits, well-bedded limestones and dolomites, crop out near Bol. The medium thick-bedded Coniacian and Santonian-Campanian limestones with dolomite intercalations are widely distributed over the island, whereas the youngest (Maastrichtian) deposits are confined to the north-western coast. The Paleogene deposits with the record of the K-Pg tsunami (Korbar et al., 2017) crop out along the north-western and, as scattered outcrops, along the south-eastern coast of the island. According to the geological maps of Borović et al. (1976), Marinčić et al. (1971, 1975, 1976), the main structure is an asymmetric fold that stretches practically from the western to the eastern coast. The northern fold limb dominating the island consists of horizontal to gently dipping beds, whereas the southern fold limb is steeper. Locally overturned beds do occur in the central part of the anticline near Bol.

On the island of Hvar, the Cretaceous rocks are mostly shallow-marine limestones with some intercalations of limestones with pelagic influence (near the Cenomanian/Turonian boundary and in the Santonian/Campanian) and late-diagenetic dolomites. The middle Eocene sediments deposited above the karstified surface containing some bauxite pockets of the

Maastrichtian-Paleocene rocks (Korbar et al., 2015) are composed of foraminiferal limestones, transitional marls and flysch (Schweitzer et al., 2007). The island is elongated in the W–E direction (Fig. 3). The main tectonic features are the WNW- ESE trending anticlines, with very steep southern limbs at places (e.g., localities H11, and H12) which are even thrusted over the Middle Eocene deep-water sandstones and marls, close to Hvar town. In the northern limb, the Cenomanian to Campanian strata are generally gently dipping towards north to northwest. The most prominent fault is a thrust/reverse fault with E-W orientation starting from Stari Grad and running sub-parallel with the axis of the anticline towards the E-SE. In addition, a system of NW-SE transverse faults are running through the island.

The island of Korčula is tectonically highly disturbed (Fig. 4) as indicated by intense folding (S and SW vergent structures) and faulting (main faults run in W-E direction). Generally, the island is an anticline with asymmetric limbs (overturned in the W part of the island, Prtoljan et al., 2007). The anticline core is made of Valangian-Hauterivian dolomites, while Barremian-Albian, Cenomanian and Turonian shallow water limestones are in the limbs.

The island of Mljet consists of a thick pile (1800 m) of Kimmeridgian/Tithonian and Cretaceous (up to late Santonian) shallow-water limestone, dolomite, intra-formational breccia, signifying higher energy environment or subaerial exposure. Quaternary “lake” deposits are known from the NW part of the island (Fig. 5). The Upper Jurassic carbonates, which are mainly dolostones with rare occurrences of inter-layered limestones, crop out on the southern half of the island. Barremian - Albian deposits cover transgressively the Upper Jurassic sediments and form a near-parallel belt with them. The Albian limestones are extremely rich in fossils, unlike the intercalated dolomite layers. Upper Cretaceous deposits extend all along the northern coast of the island. They are lithologically very similar to the Lower Cretaceous deposits but can be distinguished by micro- and macrofossil content. The structural build-up of Mljet is basically simple: it is a monocline dipping toward NNE, which, however, is probably the northern limb of an overturned anticline (Fig. 5) with an axial plane off the SW shore of the island, i.e., the whole overturned southern limb is submerged under the sea. A prominent marginal thrust fault is situated south of the island which interpreted as the contact with the stable Adria (Korbar, 2009).

The characteristic structure of Vis is an ENE plunging anticlinorium (Fig. 6). The core is built of clastic sediments, gypsum and anhydrite in associations with pyroclastics, spilites and diabase of Upper Ladinian-Upper Norian age (Koch and Belak, 2003). Lower Cretaceous

(including age defined Barremian-Albian deposits) and Cenomanian shallow-water platform carbonates (limestones and dolomites) are in the limbs. The Turonian – Coniacian limestones are confined to the northern and southern coasts. The youngest deposits are of Quaternary age and are exposed in local depressions, karst poljes and beach sand dunes. From the uplifted core of the anticlinorium a system of radial faults runs towards east. The axis of the anticlinorium gently plunges (angle is about 7°) towards east (Borović et al., 1968). Faults (presented as fault zones) are mainly sub-parallel to the long axis of the island.

Sampling

The paleomagnetic samples were drilled from a number, preferably mud supported, well-bedded, and moderately tilted limestone beds with a gasoline powered drill. The cores were oriented with a magnetic compass. However, the geological conditions were not always ideal. Thus, in order to cover the sampling area as much as possible with geographically distributed sampling localities, we sometimes sampled steeply tilted beds (e.g., localities H11, H12, Table 1) or strata with textures different from the mud-supported type (Supplementary Table 1). At each locality, the geographic co-ordinates were taken with a GPS and the bedding attitude of the sampled strata was determined from several tilt measurements.

The geological maps used during the field-work were published in the 1970th (sheets of the Basic geological map of former Yugoslavia, scale 1: 100,000, Borović et al., 1976, Marinčić et al. 1971, 1975, 1976, Korolija et al., 1975a,b, Raić et al., 1980). As we were aware of changes in some age attributions or sedimentological interpretations since the 1970s, we collected hand samples from each bed drilled for paleomagnetism, in order to check the fossil content and the texture of the sediments. The microscopy examination of thin sections cut from the hand samples concerned the biostratigraphic ranges of some foraminiferal species, in a manner of more precise age attribution. Apart from the general need for updating ages, re-interpretation of ages in the Borak/Likva section of Brač island (Fig. 2. localities B1a-e) was provoked by the discovery of tsunamites (Korbar et al., 2017). This concerned the beds sampled in the geologically very important section in the 1990s (Márton et al., 2003) which even that time had been thought to contain Cretaceous-Paleocene boundary strata. That time the tsunamite layers were not recognized and the boundary had been placed within the beds containing foraminifera *Fleuryana adriatica* De Castro, Drobne & Gušić (De Castro et al., 1994), as an index fossil. Subsequent studies revealed that Paleocene foraminifera occur

below these beds and the K/Pg boundary was allocated to a bed which was interpreted as tsunamite. Therefore, the stratigraphic range of the above-mentioned species was re-defined as being Campanian up to Maastrichtian (Schlagintweit and Rashidi, 2017; Moro et al., 2018). This development induced us to re-visit the Borak/Likva section in 2017 and 2018 for taking GPS co-ordinates and hand samples for biostratigraphic study of the earlier sampled beds (Supplementary Table 1), drill the tsunamites and neighbouring beds. We also sampled new localities in Brač island which are Cenomanian-Turonian through Maastrichtian age and represent mostly mud-supported platform carbonates, with the exception of one locality which rocks were deposited on a slope (Supplementary Table 1).

On the island of Hvar, the paleomagnetic sampling localities are fairly well covering the area, except the southern shore. The reason is no access from land to the steeply dipping strata of the southern shore or the complicated tectonics, characterising the vicinity of Hvar town. Most of the sampled localities are of Cenomanian through Campanian age. As the Lower Cretaceous deposits are massive carbonates, often dolomitized and highly karstified, it was only taking a chance when we sampled two localities (H18 and H19) on both sides of the anticline in the vicinity of Jelsa (Supplementary Table 1 and Table 1).

On Korčula island, exploration for suitable localities was quite discouraging. Eventually we drilled Aptian through Maastrichtian limestones from 11 localities (Supplementary Table 1). Except two localities, they are situated near-shore, for the outcrops in the central part of the island were either strongly tectonized/re-crystallized or weathered or both.

Paleomagnetic sampling on Mljet island was greatly helped by permission to sample in protected areas, but restricted by frequent slumping or limited access from the land to outcrops (especially on the south coast). Thus, we were able to drill only three Jurassic (lowermost Cretaceous) localities, despite of the fact that Jurassic carbonates are the most widespread in the island (Fig. 5). In addition, the accessible outcrops were mostly dolomites, without intercalated limestone beds. This was unfortunate because of the unique occurrence of the Jurassic sediments on Mljet (and the not easily accessible Lastovo) among the Dalmatic islands. The Cretaceous sediments were sampled at a larger number of localities and were intended to make a "paleomagnetic bridge" between Mljet and the other Adriatic islands.

Methods of the laboratory investigations

Standard thin sections were used for sedimentological analysis and interpretation following the descriptive terminology for carbonate rocks is after Dunham (1962) and Embry and Klovan (1971). The biostratigraphic framework is based on various descriptions of benthic foraminifera (Velić, 2007; including the newest papers like Schlagintweit, 2008; Consorti et al., 2017; Schlagintweit and Rashidi, 2017, Moro et al., 2018, Granero et al., 2019) and planktonic foraminifera (Premoli Silva and Varga, 2004). Because the biostratigraphic range of some the identified species were modified from the time when the geological maps were issued, the discrepancies in age interpretation are indicated in Supplementary Table 1.

For the paleomagnetic measurements standard size specimens were cut in the laboratory from the drill cores. The natural remanent magnetization (NRM) of the specimens was measured with JR-4 and JR-5A magnetometers (AGICO, Brno) and the magnetic susceptibility using a KLY-2 kappabridge (AGICO, Brno). Next, pilot specimens were demagnetized in several steps from each locality, either by stepwise alternating field (AF) demagnetization (LDA-3A, AGICO and Demag0179, Technical University Budapest) or by thermal demagnetization (TSD-1, Schonstedt Instrument Company, Reston). Susceptibility was monitored during thermal demagnetization. According to the behaviour of the pilot specimens, the remaining samples from each locality were demagnetized with the method which was the most efficient in defining the NRM components. The demagnetization curves (Zijderveld, 1967) were analyzed for linear segments (principal component analysis, Kirschvink, 1980). Statistical evaluation on locality/site level was based on Fisher (1953) method. The components involved in the statistical evaluation were calculated typically from 4-8 demagentization steps the components were characterized by 5° MAD and the linear segments were anchored to the origin.

In order to identify the ferrimagnetic minerals, magnetic mineralogy experiments were carried out on selected specimens. These included, IRM acquisition experiments (Molspin Pulsmagnetizer) and the stepwise thermal demagnetization of the 3-component IRM (Lowrie, 1990), accompanied by susceptibility monitoring.

Paleomagnetic results

The magnetic mineralogy experiments revealed that the dominant ferrimagnetic mineral was magnetically soft. Medium hard or hard components were typically absent or

subordinate (Fig. 7). Even when present in larger proportions (e.g., B10, K8, Fig. 7), they decayed by the Curie point of magnetite or at a bit higher temperature on stepwise thermal demagnetization of the 3-component IRM. Susceptibility monitoring on thermal demagnetization of the 3-component IRM often suggested the presence of an iron sulphide, probably pyrite, which converted into magnetite or maghemite, as indicated by the often dramatic increase of the magnetic susceptibility from 400°C on.

The magnetic susceptibility was negative for all the studied localities (Fig. 8), positive values were measured only for one bed each from localities H13 and M7. At the same time the average intensity of the NRM in the natural state was very variable. It was too weak for providing reliable paleomagnetic signals for 33 localities (Supplementary Table 2). Extreme weakness of the NRM occurred also at localities otherwise providing good paleomagnetic signals (Table 1, lower number of evaluated than collected samples). NRM intensity could be extremely different between beds of the same locality or even within a single bed, which can be explained by variable conditions during deposition and the changing concentration of the fossil content.

Based on the experience with the pilot specimens, stepwise AF demagnetization was more often applied to the majority of samples than the thermal method as the former efficiently revealed the components of the NRM during the complete decay of the NRM signal (typically achieved by max. 45mT, see Fig. 9), while avoiding the risk of creating new ferrimagnetic mineral on heating (Fig. 7).

Following stepwise demagnetization, the components decaying towards to origin of the Zijderveld diagrams were combined for each locality and a locality mean direction computed. Based on them, overall-mean paleomagnetic directions were calculated before and after tilt corrections for one of the following age groups: 1 Latest Maastrichtian-Paleocene (confided to Brač island), 2. Campanian-Maastrichtian, 2. Turonian-Santonian, 3. Albian-Cenomanian, 4. Barremian-Aptian, 5. Tithonian-Berriasian (confined to Mljet island). The groups were defined so that they match as precisely as possible those already available for stable Adria and the Northern Adriatic islands. They are of different quality from statistical point of view, from the response of the ChRM to fold/tilt test and the extent of geographical distribution. Fortunately, the 2nd and 3rd groups, which are the best from paleomagnetic point of view represent all or the majority of the Central and Southern Adriatic islands.

Despite of statistically acceptable results, some localities were omitted from the evaluations on between-locality level (Table 2). The reason was mainly the closeness of the paleomagnetic direction, before tilt correction, to that of the present or to the Late Neogene-

Pliocene Earth magnetic dipole field direction at the sampling area (Table 1, localities B11, K4, H12, V16). Locality M7 (Table 1) was also disregarded because of the obviously secondary origin of the NRM (remagnetization during Late Cretaceous due to long exposure to surface weathering indicated by bauxite filling the karstic holes in the limestone). Finally, locality H11 was rejected because the thick and thin strata yielded widely different, although individually well-defined results (Fig. 10). At this locality the characteristic remanent magnetizations (ChRM) must be composite and none of the observed directions make sense either before or after tilt corrections for the Late Cretaceous in the Adriatic realm.

Discussion

The offshore External Dinarides are bordering stable Adria in the NE. This belt comprises the Adriatic islands and is subdivided into a northern, a central and a southern segment. From the northern segment high quality paleomagnetic results are available from Cres, Ist plus surrounding islets and Dugi otok islands which had been combined with those from Vis island (Márton et al., 2014), which does not belong to the northern group. In order to compare the past relative positions of the Northern and the more southern Adriatic islands, we now recombined the data relevant only to the Northern Adratic islands (Fig. 11, Table 2). The data from Vis island, relevant to the central Adriatic area, are interpreted together in terms of tectonics with the results of the present study from Brač, Hvar, Korčula and Mljet islands (Fig. 12, Table 2). The tectonic models briefly described below, will be discussed in relation to these data sets and to the one available for stable Adria (Márton et al., 2017)

According to Herak (1986) and Tari (2002), the whole coastal Dinaridic area is one unit, named Adriatic and Imbricated Adria, regarded by both authors as parts of the Adriatic Carbonate Platform. Schmid et al. (2008) separated the Northern Adriatic islands from the more southernly ones. The former were considered to belong to the High Karst Unit, overthrusting stable Adria, whereas the central and southern islands to the Dalmatian Zone, clearly separated from the High Karst Unit. More recently Schmid et al. (2020) modified the previous subdivision and outlined a Dalmatian Zone comprising all the Adriatic islands, except the NE part of Cres island. In Korbar's model (2009), the Northern Adriatic islands are parts of the Dinaridic Unit/High Karst, the islands Brač, Hvar and Korčula are included in the Dalmatian Zone/Dalmatian Karst (Adriatic NE unit), whereas the islands of Mljet and Vis belong to the Adriatic SW unit. Some authors subdivide further the SW unit, regarding Vis

island as being outside of the area affected by neotectonic deformation, while Mljet island as affected by it (Saftić et al., 2019, Prtoljan et al., 2007, Grandić et al., 2013). The question is if large scale relative movements between the units separated by the different authors have taken place during or after the Cretaceous..

The principal differences between the above models require to evaluate the paleomagnetic results from the Adriatic islands in different combinations. According to Korbar's model (2009), Brač, Hvar and Korčula islands form one group, while Mljet and Vis another. Such separation, however can not mean large scale relative movements between the two groups for post-Aptian times, since the overall-mean paleomagnetic directions for the Albian–Cenomanian (Central islands 327°/46° α_{95} 7.2°, Southern islands 324°/47° α_{95} 7.2°) on one hand and for the Turonian-Santonian (Central islands 331°/41° alpha 8°, Southern islands 336°/49° α_{95} 9.5°), on the other hand are statistically identical.

The models placing the Northern Adriatic islands to the High Karst unit and the others to the Dalmatian zone can also be tested by comparing the high quality Turonian-Santonian and the Albian-Cenomanian overall-mean paleomagnetic directions for Brač, Hvar, Korčula, Mljet and Vis with those from the Northern Adriatic islands. In this case, the lack of large scale latitudinal or rotational differences between the Northern and more Southern Adriatic Islands is also clear (Figure 13), at least from the Late Albian on. It is interesting to note that the new kinematic model by Hinsbergen et al. (2020) is in line with Márton et al.,(2014) and with the conclusions of Márton and Ćosović (2017, published as an abstract and fully documented paleomagnetically in the present paper) concerning the tectonic relationship of the chain of the Adriatic islands to stable Adria.

The lack of significant relative movement has an important implication for post-Santonian times. Namely that the CCW rotation indicated by the results from geographically localized areas (Table 2, Campanian-Maastrichtian from Hvar and Brač islands and latest Maastrichtian-Paleocene from Brač island, Table 2) must have involved the whole offshore External Dinarides.

All the above paleomagnetic results are representing sediments which were deposited after the most important Early Cretaceous tectonic event in the Adriatic realm, a regional sea-level fall manifested in regional emergence (Velić et al., 1989, Prtoljan et al., 2007) or subaqueous erosion (Márton et al, 2010). The regionally significant sedimentary hiatus is attributed to the interplay of regional tectonism and the global sea-level fall close to the Aptian-Albian boundary (e.g., Prtoljan et al., 2007). The time before this event is represented by paleomagnetic results for Tithonian-Berriasian sediments from Mljet island and

Barremian-Aptian sediments from Hvar, Korčula, Mljet and Vis islands (ChRMs maybe of late Cenomanian age) and from Cres (ChRMs must be of pre- Late Aptian age) of the Northern Adriatic islands. These data, are not suitable to decide about the relative position of the islands, but useful in relation to stable Adria and to the bordering large plates (Fig. 13).

The Tithonian results from Mljet island are interpreted as of pre-Valanginian age and are in line with the paleolatitudinal as well as the declination trends of stable Adria and are close to expected values in an African framework (Fig. 13). The Barremian-Aptian primary magnetization obtained for Cres island implies an important northward shift and CCW rotation between Berriasian and Aptian. From this time on the paleolatitudes for stable Adria and the Adriatic islands are stabilized at near-African latitudes, around 28°N. This is in line with the interpretation from independent observations, according to which the shallow water carbonates in this area were formed in warm oligotrophic seas where the production rate in the carbonate factory was very high (Schlager, 2000; Reimjer, 2016).

The paleo-declinations suggest systematic and moderate CCW rotation with respect to Africa (Fig. 13). In the light of the about 25° post-mid Eocene CCW rotation, the systematic deviation of the "Adriatic declinations" from expected African values can be due to a small CW rotation of stable Adria and the Adriatic islands with respect to Africa followed by a CCW rotation after the mid-Eocene. Such scenario had been outlined earlier for stable Adria (Márton et al., 2017) and now supported by new data for the Adriatic islands (Fig. 13). This is true despite the fact that the post-Campanian sediments from the Adriatic islands have magnetizations of post-tilting age (Table 2), as a rotation always postdates the age of the magnetization. The high paleolatitude characterizing the Paleocene-Eocene sediments from Brač island can be conceived as an additional argument for considering the CCW rotation as a very young tectonic process.

The above results document that large scale displacements are not evidenced between Stable Adria and the Adriatic islands, i.e. the paleomagnetic results support the model by Tari (2002) who considers all the Adriatic islands as the imbricated margin of Adria. She also defines an independent Dinaric carbonate platform, which is also supported by paleomagnetic results (Fig. 14).

The paleomagnetic data from the Adriatic islands (Fig. 15) prove that the structural orientations of the Central and Southern Adriatic Islands, which are different from the dominant NW-SE "Dinaric trend" is not the consequence of an extra CCW rotation but is adequately explained by the dominance of the different orientations of the compressional deformation field at different times. According to Marinčić (1997) the Adriatic islands were

exposed to intensive E-W compression at the end of the Cretaceous, NE-SW compression in the Late Eocene-Early Oligocene and finally roughly N-S compression from the end of the Neogene on and the dominant deformation phase is getting younger from NW to SE. Strike measurements at the paleomagnetic sampling localities clearly show this trend (Figure 15). Similarly to the structural pattern of the islands, the arcuate thrust front separating imbricated and Stable Adria can also be explained by the dominance of one of the above events of deformation.

Concluding remarks

The new paleomagnetic results presented in this paper cover the Central and Southern Adriatic islands, which are characterized by WSW-ENE structural trends in contrast to the dominant NW-SE trend in the External Dinarides. There are ways to account for this difference e.g. suggesting CCW rotation of the Central and Southern Adriatic area relative to the mainland (Aljinović et al., 1987), conceiving it as a distinct tectonostratigraphic unit e.g. (Schmid et al., 2008) or even separate the Central Adriatic islands from both the Northern and the Southern Adriatic islands, and consider the latter as parts of stable Adria (Korbar, 2009).
The paleomagnetic results interpreted from the Central and Southern Adriatic islands in terms of tectonics were obtained from the laboratory processing of over 1000 independently field-oriented cores representing nearly 100 geographically distributed localities from the five largest islands. The studied localities were mostly Upper Albian through Paleocene shallow water carbonates, postdating the most important sedimentary hiatus (Late Aptian-Early Albian) documented in the NE Adriatic area. Sampling of pre-Late Aptian sediments was handicapped by their absence in Brač or the heavy karstification /secondary dolomitisation on Hvar, Korčula, Mljet islands.

The best results were obtained for the Albian - Cenomanian and the Turonian - Santonian age groups for the Central (Brač, Hvar, Korčula) as well as the Southern Adriatic (Mljet and Vis) islands. They suggest that all these islands formed a tectonic entity from the Late Albian on, since their coeval overall- mean paleomagnetic directions are statistically identical.

Similar conclusion can be drawn for their relationship to the Northern Adriatic islands as well as for stable Adria. This supports the model by Tari (2002) who defined the Adriatic

islands as the imbricated margin of stable Adria, distinguishing them tectonically from the Dinaric Carbonate Platform of the mainland.

The different tectonic orientations of the Adriatic islands, which also outline the thrust front between stable and imbricated Adria, can be explained by the dominance of differently oriented structures. These were formed during the Late Cretaceous, the Late Eocene –Early Oligocene and a neotectonic phase, respectively, resulting in dominantly N-S (e.g. Cres island), in NW-SE (Ist and surrounding islets, Dugi otok island) and in WNW-ESE (Central and southern Adriatic islands) oriented structures.

Post-Santonian paleomagnetic results from Brač and Hvar islands are in line with those from stable Adria confirming that the Adriatic Carbonate Platform must have rotated in the CCW sense after the Eocene.

Acknowledgements

This work was supported by the National Development and Innovation Office of Hungary, project K 128625, and by the Croatian Scientific Foundation, Project IP 04-2019-5775 BREEMECO. We sampled in active quarries (Pučišća, Župa) thanks to M. Vlahović, mag. ing. geol. and JADRANKAMEN d.d., and Mr. Đani Nigoević from BERICA d.d. The sites from the natural protected areas were also sampled, and we would like to thank the authorities of National park Mljet and Public Institution Sea and Karst (County of Split and Dalmatia).

References

Aljinović, B., Prelogović, E., Skoko, D., 1987, Novi podaci o dubinskoj-geološkoj građi i seizmotektonski aktivnim zonama u Jugoslaviji. Geol. Vjesnik 40, 255 – 263.

Borović, I., Marinčić, S., Majcen, Ž., Magaš, N., Rafaelli, P., Mamužić, P. 1968, Tumači za listove Vis (K 33-33), Jelsa (K 33-34), Biševo (K 33-45), Svetac (K 33-32) i Jabuka (K 33-31). (Explanatory notes for sheets Vis (K 33-33), Jelsa (K 33-34), Biševo (K 33-45) Svetac (K 33-32) and Jabuka (K 33-31), Savezni geološki zavod, Beograd, 1-67.

Borović, I., Marinčić, S., Majcen, Ž., 1976, Basic geological map of Former Yugoslavia 1: 100 000, Sheet Vis, K 3-33, Geological Survey Zagreb, Federal Geological Survey Beograd.

Butler, R.F., 1992, Paleomagnetism: magnetic domains to geological terranes. Blackwell Scientific Publications, Oxford, p 319.

Channell, J. E. T., Massari, F., Benetti, A., Pezzoni, N., 1990, Magnetostratigraphy and biostratigraphy of Callovian-Oxfordian limestones from the Trento Plateau (Monti Lessini, northern Italy). Palaeogeography, Palaeoclimatology, Palaeoecology 79, 289–303.

Channell, J. E. T., Casellato, C. E., Muttoni, G., Erba, E., 2010, Magnetostratigraphy, nannofossil stratigraphy and apparent polar wander for Adria-Africa in the Jurassic-Cretaceous boundary interval. Palaeogeography, Palaeoclimatology, Palaeoecology 293, 51–75.

Cohen, K.M., Harper, D.A.T., Gibbard, P.L., Car, N., (2003; updated) The ICS International Chronostratigraphic Chart. Episodes 36, 199–204. \www.stratigraphy.org\ICSchart\ChronostratChart2021-10

Consorti, L., Villalonga, R., Caus, E., 2017, New Rotaliids (benthic Foraminifera) from the Late Cretaceous of the Pyrenees in northeastern Spain. J. Foram. Res. 47, 284–293.

Ćosović, V., Mrinjek, E., Nemec, W., Španiček, J., Terzić, K., 2018, Development of transient carbonate ramps in an evolving foreland basin. Basin Res. 30, 746-765. https://doi.org/10.1111/bre.12274

Cox, A., 1970, Latitude dependence of the angular dispersion of the geomagnetic field. Geophysical Journal of the Royal Astronomical Society 20, 253-269. https://doi.org/10.1111/j.1365-246X.1970.tb06069.x

Dimitrijević, M.D., 1982, Dinarides: An Outline of the Tectonics. Earth. Evol. Sci. 2/1, 4-23.

De Castro P., Drobne, K., Gušić, I., 1994, *Fleryana adriatica* n. gen., n. sp. (Foramininiferida) from the uppermost Maastrichtian of the Brač Island (Croatia) and some other localities on the Adriatic Carbonate Platform. Razprave IV Razreda SAZU 35/8, 129-149.

Dunham, R.J., 1962, Classification of carbonate rocks according to depositional texture, *in* Ham, W.E., ed., Classification of Carbonate Rocks. American Association of Petroleum Geologists, Memoir 1, 108–121.

Embry, A.F. III, Klovan, J.S., 1971, A Late Devonian reef tract on northeastern Banks Island, N.W.T. Bull. Can. Pet. Geol. 4, 730–781.

Enkin, R., 2003), The direction–correction tilt test: an all-purpose tilt / fold test for paleomagnetic studies. Earth & Planet. Sci. Lett. 212, 151–166.

Fisher, R.A., 1953, Dispersion on a sphere. Proceedings of the Royal Society London, 217, 295–305.

Flügel, E., 2010, Microfacies of Carbonate Rocks. Heideberg Springer, 984 pp.

Grandić, S., Kratković, I., Balić, D., 2013, Peri-Adriatic platforms proximal talus reservoir potential (part 1). Nafta 64, 147-160.

Granero, P., Robles-Salcedo, R., Lucena, G., Troya, L., Vicedo, V., 2019. Larger foraminifera and associated fauna from the Maastrichtian of the southern Valencia Prebaetic sector (E Iberian Peninsula). Treb. Mus. Geol. Barcelona 24 (2018), 55-76.

Gušić, I., Jelaska, V., 1990, Stratigrafija gornjokrednih naslaga otoka Brača u okviru geodinamske evolucije Jadranske karbonatne platforme (Upper Cretaceous stratigraphy of the Island of Brač within the geodynamic evolution of the Adriatic Carbonate platform). Djela Jugoslavenske akademije znanosti i umjetnosti (Zagreb), 69, 160 pp.

Herak, M., 1986, A new concept of geotectonics of the Dinarides. Acta Geol. Yugoslav. Acad. Sci. and Arts 699, 42 p.

Husinec, A., Jelaska, V., 2006, Relative sea-level changes recorded on an isolated carbonate platform: Tithonian to Cenomanian succession, southern Croatia. J. Sediment. Res. 76, 1120-1136.

Kastelic, V., Carafa, M.M.C., 2012, Fault slip rates for the active External Dinarides thrust-and-fold belt. Tectonics 31, TC3019, doi:10.1029/2011TC003022, 2012

Kirschvink, J.L., 1980, The least-squares line and plane and the analysis of paleomagnetic data. Geophys. J. R. Astron. Soc. 62, 699–718.

Koch, G., Belak, M., 2003, Evaporitic-carbonate deposits of Komiža diapiric structure (Island of Vis, Croatia): their palynostratigraphy and sedimentological features. In:Vlahović, I (ed.) 22nd IAS Meeting Of Sedimentology, Opatija, 17-19.09.2003, p. 96.

Korbar, T., 2009, Orogenic evolution of the External Dinarides in the NE Adriatic region: A Model constrained by tectonostratigraphy of upper Cretaceous to Paleogene carbonates. Earth-Sci. rev. 96, 296 – 312.

Korbar, T., Belak, M., Fuček, L., Husinec, A., Oštrić, N., Palenik, D., Vlahović, I., 2012. Basic Geological Map of the Republic of Croatia 1:50000. Sheets Vis 3 and Biševo 1 with Part of the Sheet Vis 4 and Islands Sv Andrija, Brusnik, Jabuka and Palagruža. Croatian Geological Survey: Zagreb.

Korbar, T., Montanari, A., Premec Fućek, V., Fuček, L., Coccioni, R., McDonald, I., Claeys, P., Schulz, T., Koeberl, C., 2015, Potential Cretaceous – Paleogene boundary tsunami deposit in the intra-Tethyan Adriatic Carbonate Platform section of Hvar (Dalmata, Croatia). Geol. Soc. America Bull. 127, 1666 – 1680.

Korbar. T., McDonald, I., Premec Fućek, V., Fuček, L., Posilović, H., 2017, Post-impact event bed (Tsunamite) at the Cretaceous – Palaeogene boundary deposited on a distal carbonate platform interior. Terra Nova 29, 135-143.

Korolija, B., Borović, I., 1975a, Basic geological map of Former Yugoslavia 1:100 000, Sheet Lastovo, K 33-46 and 57. Geological Survey Zagreb, Federal Geological Survey Beograd.

Korolija, B., Borović, I., Grimani, I., Marinčić, S., 1975b, Basic geological map of former Yugoslavia, Sheet Korčula 1: 100 000, K 33-47. Geological Survey Zagreb, Federal Geological Survey Beograd.

Lowrie, W., 1990, Identification of feromagnetic minerals in a rock by coercitive and unblocking temperature properties. Geophys. Res. Lett. 17, 159–162.

Marinčić, S., 1997, Tectonic Structure of the Island of Hvar (Southern Croatia). Geol. Croat. 50/1, 57 - 77.

Marinčić, S., Majcen, Ž., 1975 (1976), Basic geological map of former Yugoslavia 1: 100 000, Sheet Jelsa, K 33-34. Geological Survey Zagreb, Federal Geological Survey Beograd.

Marinčić, S., Korolija, B., Majcen, Ž., 1976, Basic geological map of Former Yugoslavia 1: 100 000, Sheet Omiš, K 33-22. Geological Survey Zagreb, Federal Geological Survey Beograd.

Marinčić, S., Magaš, N., Borović I., 1971, Basic geological map of Former Yugoslavia 1:100 000, Sheez Split, K 33-21. Geological Survey Zagreb, Federal Geological Survey Beograd.

Márton. E., Ćosović, V. 2017: Inconsistent tectonic trends, consistent paleomagnetic directions: an example from External Dinarides.
EGU series – Émile Argand Conference, 13th Workshop on the Alpine Geological Studies, Zlatibor, Serbia. 13th Workshop on the Alpine Geological Studies Abstract Volume (ISBN 978-86-7352-297-5), 64.

Márton, E., Moro, A., 2009, New paleomagnetic results from imbricated Adria: Ist Island and related areas. Geol. Groat. 62/2, 107–114.

Márton, E., Drobne, K., Ćosović, V., Moro, A., 2003, Palaeomagnetic evidence for Tertiary counterclockwise rotation of Adria. Tectonophysics 377/1-2, 143–156.

Márton, E., Ćosović, V., Moro, A., Zvocak, S., 2008, The motion of Adria during the Late Jurassic and Cretaceous: New paleomagnetic results from stable Istria. Tectonophysics 454/1-4, 44–53.

Márton, E., Zampieri, D., Grandesso P., Ćosović, V., Moro, A., 2010, New Cretaceous paleomagnetic results from the foreland of the Southern Alps and the refined apparent polar wander path for stable Adria. Tectonophysics 480, 57-72.

Márton, E., Zampieri, D., Kázmér, M., Dunkl, I., Frisch, W., 2011, New Paleocene–Eocene paleomagnetic results from the foreland of the Southern Alps confirm decoupling of stable Adria from the African plate. Tectonophysics 504, 89-99.

Márton, E., Ćosović, V., Moro, A., 2014, New stepping stones, Dugi otok and Vis islands, in the systematic paleomagnetic study of the Adriatic region and their significance in evaluations of existing tectonic models. Tectonophysics 611, 141-154. https://doi.org/10.1016/j.tecto.2013.11.016

Márton, E., Zampieri, D., Ćosović, V., Moro, A., Drobne, K., 2017, Apparent Polar Wander Path for Adria extended by new Jurassic paleomagnetic results from its stable core: tectonic implications. Tectonophysics 700-701, 1-18. https://doi.org/10.1016/j.tecto.2017.02.004

McFadden, P.L., McElhinny, M. W., 1990, Classification of the reversal test in palaeomagnetism. Geophys. J. Int. 103, 725–729.

McFadden, P.L., McElhinny, M. W., 1988, The combined analysis of remagnetization circles and direct observations in paleomagnetism. Earth Planet. Sci. Lett. 87, 161-172.

Moro, A., Ćosović, V., 2013, Upper Turonian–Santonian slope limestones of the Islands of Premuda, Ist and Silba (Adriatic Coast, Croatia). Geol. Croat. 66/1, 1-13.

Moro, A., Velić, I., Mikuž, V., Horvat, A., 2018, Microfacies characteristics of carbonate cobble from Campanian of Slovenj Gradec (Slovenia): implications for determining *Fleuryana adriatica* De Castro, Drobne and Gušić paleoniche and extending the biostratigraphic range in the Tethyan realm. Rud.-geol.-naft. zb. 33/4, https://doi.org/10.17794/rgn.2018.4.133/4

Muttoni, G., Dallanave, E., Channell, J. E. T., 2013, The drift history of Adria and Africa from 280 Ma to Present, Jurassic true polar wander, and zonal climate control on Tethyan sedimentary facies, Palaeogeography, Palaeoclimatology, Palaeoecology 386, 415–435.

Pamić, J., Gušić, I., Jelaska, V., 1998, Geodynamic evolution of the Central Dinarides. Tectonophysics 297, 251-268.

Picha, F.J., 2002, Late orogenic strike-slip faulting and escape tectonics in frontal Dinarides-Hellenides, Croatia, Yugoslavia, Albania and Greece. AAPG Bulletin 86/9, 1659-1671.

Placer, L., Vrabec, M., Celarc, B., 2010, The basis for understanding of the NW Dinarides and Istria Peninsula tectonics. Geologija 53/1, 55-86.

Premoli Silva, I., Verga, D., 2004, Practical manual of Cretaceous planktonic foraminifera. In D. Verga, R. Rettori (Eds.), International School on Planktonic Foraminifera: Perugia, Italy, Tipografia Ponte Felcino, Universities of Perugia and Milan, 3rd Course, p. 283

Prtoljan, B., Jamičić, D., Cvetko Tešović, B., Kratković, I., Markulin, Ž., 2007, The influence of Late Cretaceous synsedimentary deformation on the Cenozoic structuration of the middle Adriatic, Croatia. Geodin. Acta 20/5, 287-300.

Raić. V., Papeš, J., Ahac, A., Korolija, B., Grimani, I, Marinčić, S, 1980, Basic geological map of former Yugoslavia, sheet Ston 1: 100 000 K33-48, Geological Survey, Sarajevo, Geological Survey, Zagreb.

Reijmer, J.J.G., 2016, Carbonate Factories. In: Harff, J., Meschede, M., Petersen, S., Thiede, J. (eds.), Encyclopedia of Marine Geosciences. Encyclopedia of Earth Sciences Series. Springer, Dordrecht. https://doi.org/10.1007/978-94-007-6238-1_136

Saftić, B., Kolenković, I., Cvetković, M., Vulin, D., Velić, J., Tomljenović, B., 2019, Potential for the Geological Storage of CO_2 in the Croatian Part of the Adriatic Offshore. Minerals, 9, 577; doi:10.3390/min9100577

Schlager, W., 2000, Sedimentation rates and growth potential of tropical, cold water and mud mound carbonate systems. In: Insalaco, E., Skelton, P.W., Palmer, T.J. (eds.), Carbonate Platform Systems: components and interactions. Geological Society London Spec. Publ., 178, 217-227.

Schlagintweit, F., 2008, Reassessment of *"Nummoloculina" regularis* Philippson, 1887, a benthic foraminifer from the Upper Cretaceous of the Northern Calcareous Alps, Austria. Neues Jahrb. Geol. Paläontol. – Abh. 248/1, 115–122.

Schlagintweit, F., Rashidi, K., 2017, Some new and poorly known benthic foraminifera from Late Maastrichtian shallow-water carbonates of the Zagros zone, SW Iran. Acta Palaeontol. Rom. 12/1 (2016), 53-70.

Schmid, S. M., Bernoulli, D., Fügenschuh, B., Matenco, L., Schefer, S., Schuster, R., Tischler, M., Ustaszewski, K., 2008, The Alpine-Carpathian-Dinaridic orogenic system: correlation and evolution of tectonic units. Swiss J. Geosci. 101/1, 139-183.

Schmid S.M., Fügenschuh, B., Kounov, A., Matenco, L., Nievergelt, P., Oberhansli, R., Pleuger, J., Schelfer, S., Schuster, R., Tomljenović, B., Ustaszewski, K., van Hinsbergeen, D.J.J., 2020, Tectonic units of Alpine collision zone between eastern Alps and western Turkey. Gondwana research 78, 308-374.

Schweitzer, C., Shirk, A., Ćosović, V., Okan, Y., Feldmann, R., Hosgor, I., 2007, New species of Harpactocarcinus from the Tethyan Eocene and their paleoecological setting. J. Paleontol. 81/5, 1091-1100.

Šumanovac, F., Markušić, S., Engelsfeld, T., Jurković, K.. Orešković, J., 2017, Shallow and deep lithosphere slabs beneath the Dinarides from teleseismic tomography as the result of the Adriatic lithosphere downwelling. Tectonophysics 712/713, 523-541.

Tari, V., 2002, Evolution of the northern and western Dinarides; a tectonostratigraphic approach. EGS Stephan Mueller Special Publisher Series, 1, 1-21.

Tauxe, L., Kent, D.V., 2004, A simplified statistical model for the geomagnetic field and the detection of shallow bias in paleomagnetic inclinations: was the ancient magnetic field dipolar? in: J.E.T. Channell, D.V. Kent, W. Lowrie, J.G. Meert (Eds.), Timescales of the Paleomagnetic Field, AGU Monograph. American Geophysical Union, Washington, DC.

Tomljenović, B., Csontos, L., Marton, E., Marton P., 2008, Tectonic evolution of the northwestern Internal Dinarides as constrained by structures and rotation of Medvednica Mountains, North Croatia. Geological Society, London, Special Publications, 298, 145-167, https://doi.org/10.1144/SP298.8

Torsvik, T. H., Van der Voo, R., Preeden, U., Mac Niocaill, C., Steinberger, B., Doubrovine, P. V., Van Hinsbergen, D. J. J., Domeier, M., Gaina, C., Tohver, E., Meert, J. G., McCausland, P. J. A., Cocks, L. R. M., 2012, Phanerozoic polar wander, paleogeography and dynamics. Earth Science Review 114, 325-368.

van Hinsbergen, D. J. J., Torsvik, T. H., Schmid, S. M., Matenco, L. C., Maffione, M., Vissers, R. L. M., Gürer, D., Spakman, W., 2020, Orogenic architecture of the Mediterranean region and kinematic reconstruction of its tectonic evolution since the Triassic. Gondwana Res. 81, 79-229. https://doi.org/10.1016/j.gr.2019.07.009

Velić, I., Tišljar, J., Sokač, B., 1989, The variability of thickness of the Barremian, Aptian and Albian carbonates as a consequence of changing depositional environments and emersions in western Istria (Croatia, Yugoslavia). Mem. Soc. Geol. It. 40, 209-218.

Velić, I., 2007, Stratigraphy and Palaeobiogeography of Mesozoic Benthic Foraminifera of the Karst Dinarides (SE Europe). Geol. Croat. 60/1, 1-113

Vlahović, I., Tišljar, J., Velić, I., Matičec, D., 2005, Evolution of the Adriatic carbonate Platform: Palaeogeography, main events and depositional dynamics. Palaeogeogr. Palaeoclimatol. Palaeoecol. 220, 333-360.

Zijderveld, J.D.A., 1967, A.C. demagnetization of rocks: Analysis of results. In: Methods in palaeomagnetism, eds. D.V. Collinson, K.M. Creer and S.K. Runcorn, Elsevier, Amsterdam, pp. 254–286.

Figure captions

Fig. 1 Simplified tectonic map of the Dinarides and adjacent regions, showing the subdivision of the Dinarides (modified after Placer et al., 2010) and the areas of the paleomagnetic investigations (Published results are from Adige embayment and stable Istria (Márton et al., 2017) , from Cres, from Ist and surrounding islets and from Dugi otok, all belonging to the Northern Adriatic islands (Márton et al., 2014) and the targets of the present study: Brač, Hvar, Korčula, Mljet and Vis islands of the Central Adriatic area.

Fig. 2 Simplified geological map of the island of Brač (modified after Borović et al., 1976; Marinčić et al., 1971, 1975, 1976) with the locations of collected paleomagnetic cores and biostratigraphic samples.
Keys: 1a - h= Borak/Likva at Sutivan, 2= Postire, 3= Mirca, 4= Sumartin, 5= Splitska, 6= Nerežišća, 7= road to Pučišća quarry, 8 a - d= Pučišća quarry; 9= Gračišće, 10= Planica, 11= Hunčac, 12= Grška bay, 13= Grižev promontory, 14= Milna (Olive grove), 15= Vidova gora, 16= Bol (Sv. Duh), 17= Maslinova Milna, 18= Zagvozd.

The tectono-stratigraphic legend: **1** $E_{1,2}$ Lower – Middle Eocene; **2** Pc, E Paleocene, Eocene; **3** $^{3}K^{3}{}_{2}$ Campanian; **4** $^{2}K^{3}{}_{2}$ Santonian; **5**. $K^{2}{}_{2}$ Turonian; **6** Local faults; **7** Faults; **8** Traces of axial planes of major anticlines; **9** Strike and dip of strata.

Fig. 3 Simplified geological map of the island of Hvar (modified after Borović et al., 1976; Marinčić et al., 1971, 1975, 1976) with the locations of collected paleomagnetic cores and biostratigraphic samples. Keys: 1= Perna bay; 2= Zaglav, 3= Poljica – Stiniva (close to the road), 4= Poljica – Stiniva, 5= Nova Crkva, 6= Lozna bay, 7= Maslinica bay, Vrbovska, 8= Brusje, Stiniva bay, 9= Vira I bay, 10= Vira II bay, 11= Gromin dolac, 12= Soča bay, 13= Križišće, 14= Rudine, 15= Basina, 16= Zavala bay, 17= Bristova, 18= Jelsa, 19= Pitve.
The tectono-stratigraphic legend: **1** $E_{2,3}$ Middle – Upper Eocene; **2** $E_{1,2}$ Lower – Middle Eocene; **3** $^{3}K^{3}{}_{2}$ Maastrichtian; **4** $^{1+2}K^{3}{}_{2}$ Coniacian and Santonian- Campanian; **5** $K^{2}{}_{2}$ Upper Turonian; **6** $K^{1,\ 2}{}_{2}$ Cenomanian-Turonian; **7** $^{2}K_{1}$ Albian; **8** $^{1}K_{1}$ Lower Cretaceous; **9** Traces of axial planes of major overturned anticline and anticline; **10** Fault; **11** Strike and dip of strata.

Fig. 4 Simplified geological map of the island of Korčula (modified after Korolija et al. 1975a, b) with locations of collected paleomagnetic cores and biostratigraphic samples. Keys: 1 = Samograd – Račišće, 2 = Prižba, 3 = Karbuni-2, 4 = Blaca-2, 5 = Grščica, 6 = Karbuni-1, 7 = Gornja Potira, 8 = Zavalatica, 9 = Blaca, 10 = Babina, 11 = Babina Smokva.
The tectono-stratigraphic legend: **1** Quaternary; **2** $K^{3}{}_{2}$ Coniacian – Maastrichtian; **3** $K^{1+2}{}_{2}$ Cenomanian – Turonian; **4** $K^{2}{}_{2}$ Turonian; **5** $K^{1}{}_{2}$ Cenomanian; **6** $K^{3\text{-}5}{}_{1}$ Barremian - Albian; **7** $K^{1+2}{}_{1}$ Lower Cretaceous; **8** Traces of axial planes of major (synclines and anticlines); **9** Faults (normal and reverse); **10** Strike and dip of strata.

Fig. 5 Simplified geological map of the island of Mljet (modified after Raić et al., 1980) with the locations of collected paleomagnetic cores and biostratigraphic samples. Keys: 1 = Maranovići, 2 = Požura – 2, 3 = Okuklja bay, 4 = Požura – 1, 5 = Blato, 6 = Saplunara, 7 = Paselo, 8 = Vrata Soline, 9 = Sobra, 10 = Pomena 1 + 2, 11 = Punta Križa, 12 = Kozarica, 13 = Lokve bay, 14 = Sutmiholjska bay.
The tectono-stratigraphic legend: **1** $K^{2}{}_{2}$ Turonian - Early Coniacian; **2** $K^{1}{}_{2}$ Lower part of the Upper Cretaceous; **3** $K^{5}{}_{1}$ Albian; **4** $K^{3\text{-}5}{}_{1}$ Barremian – Albian; **5** $J^{3}{}_{3}$ Upper part of the Upper Jurassic; **6** $J^{2,3}{}_{3}$ Upper Jurassic; **7** Faults; **8** Traces of axial planes of major overturned anticlines; **9** Strike and dip of strata.

Fig. 6 Simplified geological map of the island of Vis (simplified after Korbar et al., 2012) with the locations of collected paleomagnetic cores and biostratigraphic samples. Keys: 1 = Titova Spilja, 2 = Mali Hum 1, 3 = Mali Hum 2, 4 = Sv. Mihovil, 5 = Kupinovac, 6 = Stupišče, 7 = Vis, Hotel Issa, 8 = Vis Town, Bandirica, 9 = Vis Town, 10 = Dragodir, 11 = Vis, Grandovac, 12 = Rogačića, 13 = Parja, 14 = Promontory Parja, 15 = Uvala Tiha, 16 = Oključna 1, 17 = Oključna 2, 18 = Rukavac 1, 19 = Rukavac 2, 20 = Srebrna 1, 21 = Srebrna 2, 22 = Srebrna bay, 23 = Tremule, 24 = Mala Travna Uvala.
The tectono-stratigraphic legend: **1** Quaternary deposits; **2** Turonian-Coniacian limestones; **3** Cenomanian dolomites and limestones; **4** Lower Cretaceous limestones; **5** Lower Cretaceous dolomites; **6** Triassic volcanogenetic-sedimentary-evaporitic complex; **7** Faults; **8** Strike and dip of strata.

Fig. 7 Identification of the magnetic minerals (method by Lowrie, 1990) in Cretaceous platform limestones from Brač, Hvar, Mljet and Korčula islands.
From top to bottom: IRM acquisition, thermal demagnetization of the 3-component IRM, susceptibility after each demagnetization steps. The components of the IRM were acquired in fields of 1.0 T (squares), 0.36 T (full circles) and 0.12 T (open circles).

Fig. 8 Upper Jurassic through Lower Eocene carbonates of the NE Adriatic Carbonate Platform. Magnetic susceptibility vs. NRM intensity diagram based on locality mean values for the Central and Southern Adriatic islands.

Fig. 9 Typical demagnetization curves for platform limestones of Brač, Hvar, Korčula and Mljet islands. Key: Zijderveld diagrams (Zijderveld, 1967) in geographic system. In case of AF demagnetization they are accompanied by intensity (circles) versus demagnetizing field diagrams, and by NRM intensity (circles)/susceptibility (dots) v.s. temperature diagrams, when the method is thermal (TH) demagnetization. In the Zijderveld diagrams full dots are the projections of the NRM vector onto the horizontal; circles: into the vertical.

Fig. 10 Gromin Dolac (locality H11): ChRM directions from thin (squares) the thick (diamonds) beds before (a) and after (b) tilt correction. Stereographic projection, full symbols: positive, empty symbols: negative inclinations. C and d are the results of magnetic mineralogical experiments on samples with widely different NRM intensities. The ChRMs of the thin beds are probably the resultants of a CCW rotated remanence overprinted during a reversed polarity Chron, post-dating the CCW rotation (see the ChRMs of relatively close localities: K4 and H12), and eventually overprinted in the present Earth magnetic field. The ChRMs of the thick beds (over one meter) must be the resultants of a normal and reversed polarity remanence. For key see Fig.7).

Fig. 11 Fold/tilt tests for the Northern Adriatic Islands Paleomagnetic locality mean directions (squares) and the overall-mean direction (dot) with α_{95} on stereographic plots (positive inclinations: full, negative inclination: empty symbols) before (left) and after (right) tilt corrections, accompanied by the results of the tilt test (in the middle) for the Turonian-Santonian (11 a-c), for the Albian-Cenomanian (11 d-f) and for the Barremian-Aptian (11 g-i).

Fig. 12 Fold/tilt tests for the Central and Southern Adriatic islands. Paleomagnetic locality mean directions (squares) and the overall-mean direction (dot) with α_{95} on stereographic plots (positive inclinations: full, negative inclination: empty symbols) before (left) and after (right) tilt corrections, accompanied by the results of the tilt test (in the middle) for the Campanian-Maastrichtian (12 a-c), for the Turonian-Santonian (12 d-f) and the Albian-Cenomanian (12 g-i) carbonates. The test is indeterminate for the first and third age groups which were affected by well-documented syn-sedimentary tectonics during the Late Cenomanian and the Maastrichtian, respectively, while the deposition of the Turonian-Santonian carbonates took place during a tectonically quiet period (Prtoljan et al., 2007).

Fig. 13 Paleolatitudes and paleodeclinations for the NE part of the Adriatic region (stable Adria, Márton et al., 2017, Northern Adriatic islands, Márton et al., 2014, Central and southern Adriatic islands, present study) compared with those expected for stable Europe and Africa (Global APWP, Torsvik et al., 2012), respectively. The error bars for the paleomagnetic results are based on number of independently oriented samples (left side) and alternatively on the number of localities (right side). The error bars were computed based on Butler (1992). The geological age groups in the coloured bar are 1 = Priabonian – Lutetian, 2 = Paleocene – Ypresian, 3 = Campanian–Maastrichtian, 4 = Turonian–Santonian, 5 = Albian–Cenomanian, 6 = Barremian–Aptian, 7 = Valanginian–Hauterivian, 8 = Tithonian–Berriasian, 9 = Oxfordian–Tithonian, 10 = Callovian–Oxfordian, 11 = Bajocian-Bathonian. Lighter squares represent magnetization of post tilting age.

Fig. 14 Comparison of paleomagnetic overall-mean directions for Middle Jurassic-Earliest Cretaceous for stable Adria and for Mljet island, on one hand, and for rocks of similar ages from the High Karst between Rijeka and Zadar (stereographic plot, lower hemisphere).

Fig. 15 The general tectonic subdivision of the NE part of the Adriatic region after Tari (2002) with Turonian-Santonian paleomagnetic declinations (arrows with statistical errors) illustrate the lack of relative movements between the islands and with respect to stable Adria, which is proved by all paleomagnetic data after the Late Aptian-Early Albian tectonic event. The arcuate shape of imbricated Adria is explained by the dominance of one of the three main compressional regime of different orientations, getting younger from NW to SE (Marinčić, 1997). The rose diagrams based on our strike measurements in the field are presented to show that the tectonic strikes reflect in Cres island the dominance of the uppermost Cretaceous Laramian (N-S), in Ist and Dugi Otok islands the mid-Eocene-Oligocene (NW-SE) and (in the Central and Southern Adriatic the neotectonic phase (WNW-ESE) tectonic structures.

Tables

Table 1. Brač, Mljet, Korčula, Hvar and Vis islands. Summary of locality mean palaeomagnetic directions based on the results of principal component analysis (Kirschvink 1980), except localities B17, H5, H10 and V23, where combination of stable end points and demagnetization circles was used (McFadden and McElhinny 1988).
Key: Lat.N, Lon.E: Geographic coordinates (WGS84) measured by GPS, n/no: number of used/collected samples (the samples are independently oriented cores); D, I (Dc, Ic): declination, inclination before (after) tilt correction; k and α_{95}: statistical parameters (Fisher 1953); Paleo lat: paleolatitude; Pole lat and Pole long: coordinates of the paleopole; δm, δp: statistical parameters of the palaeomagnetic pole. *: post-tilting magnetization, pole calculated from directions before tilt correction; **: rejected from tectonic interpretation, very young remagnetization, poles not calculated.

Table 2. Summary of the overall mean paleomagnetic directions before and after tilt corrections, results of direction correction tilt test (Enkin, 2008) and paleomagnetic

poles with statistical parameters. Key as for Table 1. but N is the number of localities. * E/I corrected (Tauxe and Kent, 2004).

Supplementary Table 1. The complete list of sampled locations on Brač, Hvar, Korčula and Mljet islands. Each location is correlated with the location number, the age attribution (after geological maps and references Velić, 2007; Schlagintweit, 2008; Consorti et al., 2017; Schlagintweit and Rashidi, 2017; Moro et al., 2018; Granero et al., 2019) and the sedimentary texture (after Dunham, 1962, modified by Embry and Klovan, 1971) and Flügel (2010).

Supplementary Table 2. List of the localities providing no paleomagnetic result, mainly due to extremely weak NRM.

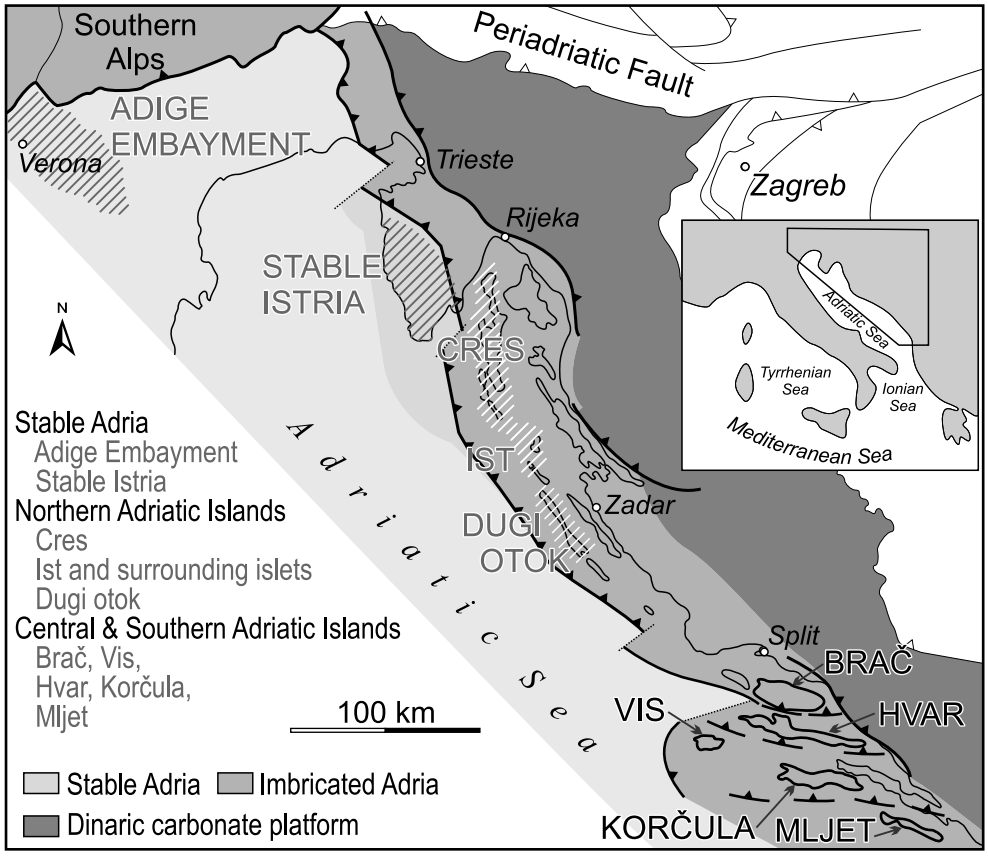

Fig. 1 Simplified tectonic map of the Dinarides and adjacent regions, showing the subdivision of the Dinarides (modified after Placer et al., 2010) and the areas of the paleomagnetic investigations (Published results are from Adige embayment and stable Istria (Márton et al., 2017) , from Cres, from Ist and surrounding islets and from Dugi otok, all belonging to the Northern Adriatic islands (Márton et al., 2014) and the targets of the present study: Brač, Hvar, Korčula, Mljet and Vis islands of the Central Adriatic area.

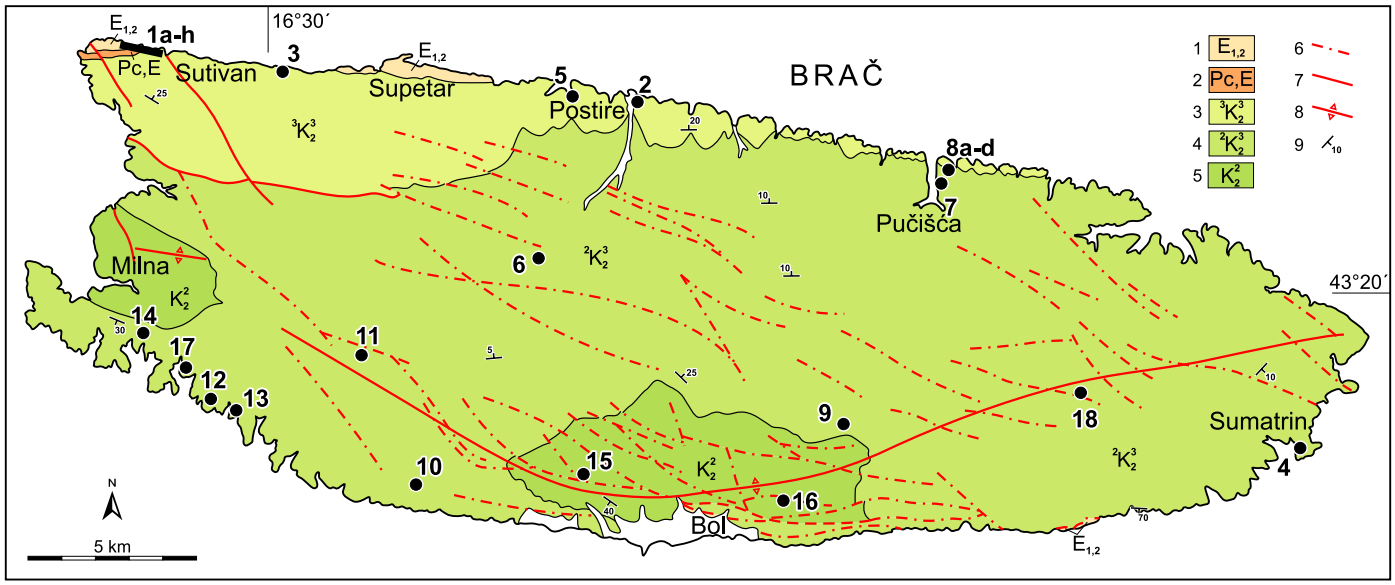

Fig. 2 Simplified geological map of the island of Brač (modified after Borović et al., 1976; Marinčić et al., 1971, 1975, 1976) with the locations of collected paleomagnetic cores and biostratigraphic samples.
Keys: 1a - h= Borak/Likva at Sutivan, 2= Postire, 3= Mirca, 4= Sumartin, 5= Splitska, 6= Nerežišća, 7= road to Pučišća quarry, 8 a - d= Pučišća quarry; 9= Gračišće, 10= Planica, 11= Hunčac, 12= Grška bay, 13= Grižev promontory, 14= Milna (Olive grove), 15= Vidova gora, 16= Bol (Sv. Duh), 17= Maslinova Milna, 18= Zagvozd.
The tectono-stratigraphic legend: **1** $E_{1,2}$ Lower – Middle Eocene; **2** Pc, E Paleocene, Eocene; **3** $^{3}K^{3}_{2}$ Campanian; **4** $^{2}K^{3}_{2}$ Santonian; **5**. K^{2}_{2} Turonian; **6** Local faults; **7** Faults; **8** Traces of axial planes of major anticlines; **9** Stike and dip of strata.

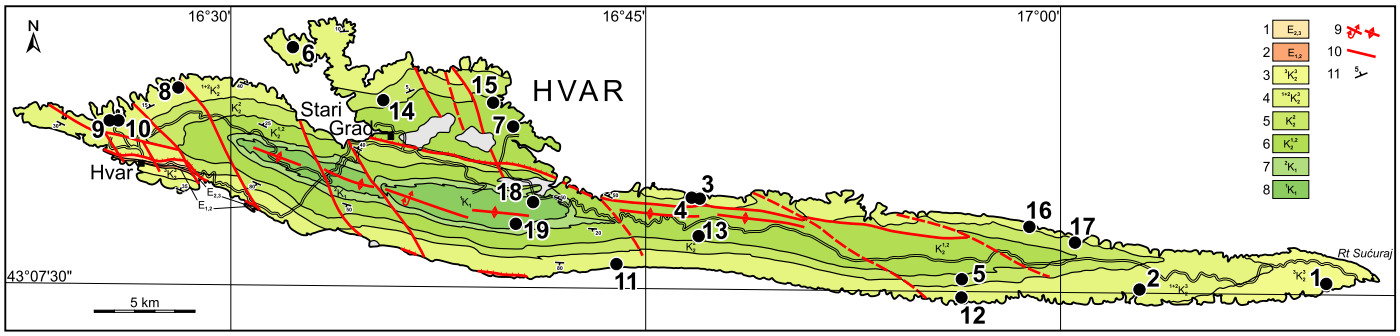

Fig. 3 Simplified geological map of the island of Hvar (modified after Borović et al., 1976; Marinčić et al., 1971, 1975, 1976) with the locations of collected paleomagnetic cores and biostratigraphic samples. Keys: 1= Perna bay; 2= Zaglav, 3= Poljica – Stiniva (close to the road), 4= Poljica – Stiniva, 5= Nova Crkva, 6= Lozna bay, 7= Maslinica bay, Vrbovska, 8= Brusje, Stiniva bay, 9= Vira I bay, 10= Vira II bay, 11= Gromin dolac, 12= Soča bay, 13= Križišće, 14= Rudine, 15= Basina, 16= Zavala bay, 17= Bristova, 18= Jelsa, 19= Pitve.

The tectono-stratigraphic legend: **1** $E_{2,3}$ Middle – Upper Eocene; **2** $E_{1,2}$ Lower – Middle Eocene; **3** $^{3}K^{3}_{2}$ Maastrichtian; **4** $^{1+2}K^{3}_{2}$ Coniacian and Santonian- Campanian; **5** K^{2}_{2} Upper Turonian; **6** $K^{1,2}_{2}$ Cenomanian-Turonian; **7** $^{2}K_{1}$ Albian; **8** $^{1}K_{1}$ Lower Cretaceous; **9** Traces of axial planes of major overturned anticline and anticline; **10** Fault; **11** Strike and dip of strata.

Fig 4.

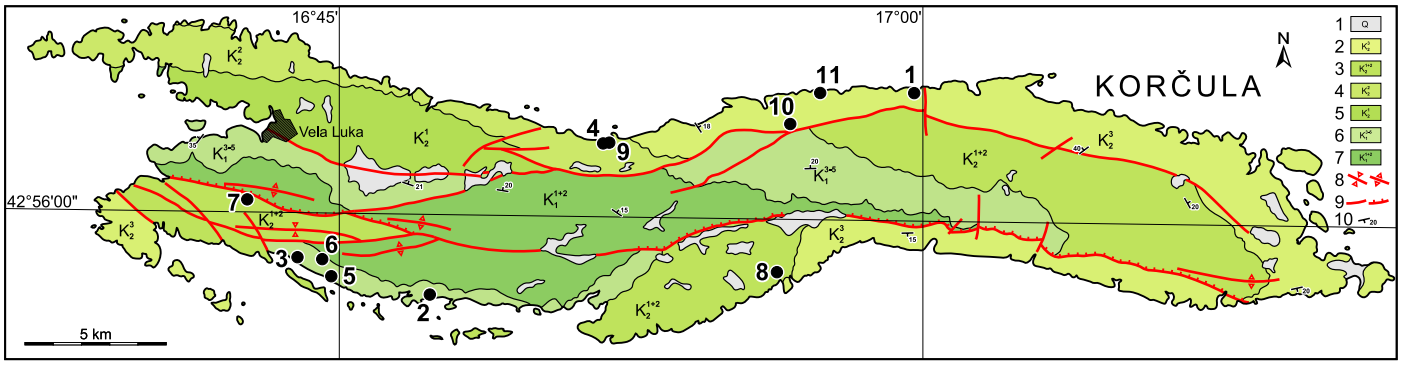

Fig. 4 Simplified geological map of the island of Korčula (modified after Korolija et al. 1975a, b) with locations of collected paleomagnetic cores and biostratigraphic samples. Keys: 1 = Samograd – Račišće, 2 = Prižba, 3 = Karbuni-2, 4 = Blaca-2, 5 = Grščica, 6 = Karbuni-1, 7 = Gornja Potira, 8 = Zavalatica, 9 = Blaca, 10 = Babina, 11 = Babina Smokva.

The tectono-stratigraphic legend: **1** Quaternary; **2** K^{3}_{2} Coniacian – Maastrichtian; **3** K^{1+2}_{2} Cenomanian – Turonian; **4** K^{2}_{2} Turonian; **5** K^{1}_{2} Cenomanian; **6** K^{3-5}_{1} Barremian - Albian; **7** K^{1+2}_{1} Lower Cretaceous; **8** Traces of axial planes of major (synclines and anticlines); **9** Faults (normal and reverse); **10** Strike and dip of strata.

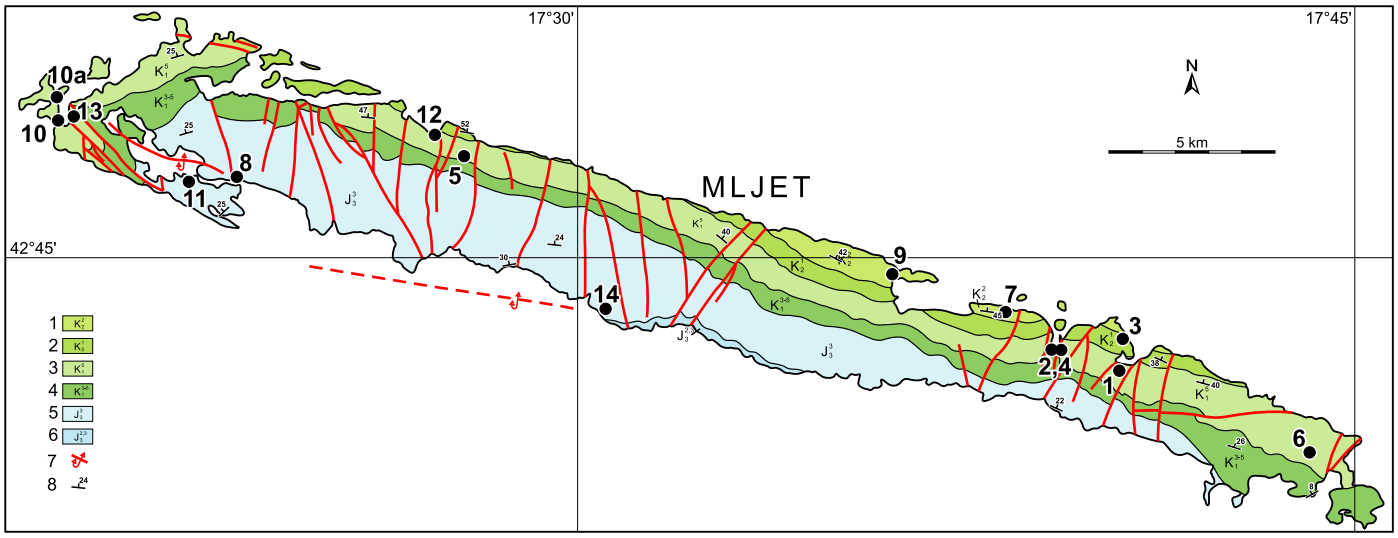

Figure 5: Simplified geological map of the island of Mljet (modified after Raić et al., 1980) with location of collected paleomagnetic cores and biostratigraphic samples. Keys: 1 = Maranovići, 2 = Požura – 2, 3 = Okuklja bay, 4 = Požura – 1, 5 = Blato, 6 = Saplunara, 7 = Paselo, 8 = Vrata Soline, 9 = Sobra, 10 = Pomena 1 + 2, 11 = Punta Križa, 12 = Kozarica, 13 = Lokve bay, 14 = Sutmiholjska bay.
The tectono-stratigraphic legend: **1** K^{2}_{2} Turonian - Early Conacian; **2** K^{1}_{2} Lower part of the Late Cretaceous; **3** K^{5}_{1} Albian; **4** $K^{3\text{-}5}_{1}$ Barremian – Albian; **5** J^{3}_{3} Upper part of the late Jurassic; **6** $J^{2,3}_{3}$ Late Jurassic; **7** Trace of axial plane; **8** Traces of axial planes of major overturned anticlines; **9** Strike and dip of strata.

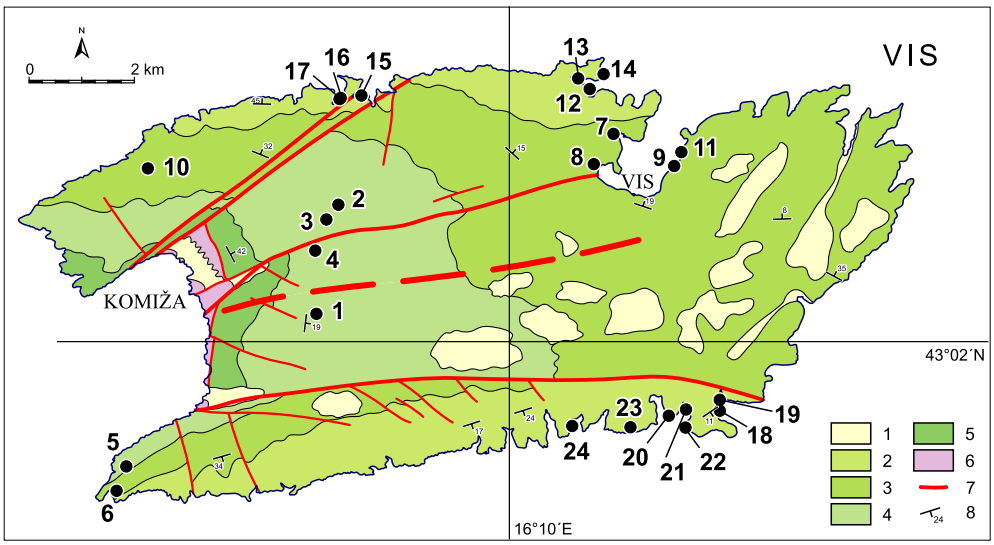

Fig. 6 Simplified geological map of the island of Vis (simplified after Korbar et al., 2012) with the locations of collected paleomagnetic cores and biostratigraphic samples. Keys: 1 = Titova Spilja, 2 = Mali Hum 1, 3 = Mali Hum 2, 4 = Sv. Mihovil, 5 = Kupinovac, 6 = Stupišče, 7 = Vis, Hotel Issa, 8 = Vis Town, Bandirica, 9 = Vis Town, 10 = Dragodir, 11 = Vis, Grandovac, 12 = Rogačića, 13 = Parja, 14 = Promontory Parja, 15 = Uvala Tiha, 16 = Okljućna 1, 17 = Okljućna 2, 18 = Rukavac, 19 = Rukavac, 20 = Srebrna, 21 = Srebrna, 22 = Srebrna bay, 23 = Tremule, 24 = Mala Travna Uvala.
The tectono-stratigraphic legend: 1 Quaternary deposits; 2 Turonian-Coniacian limestones; 3 Cenomanian dolomites and limestones; 4 Lower Cretaceous limestones; 5 Lower Cretaceous dolomites; 6 Triassic volcanogenetic-sedimentary-evaporitic complex; 7 Faults; 8 Strike and dip of strata.

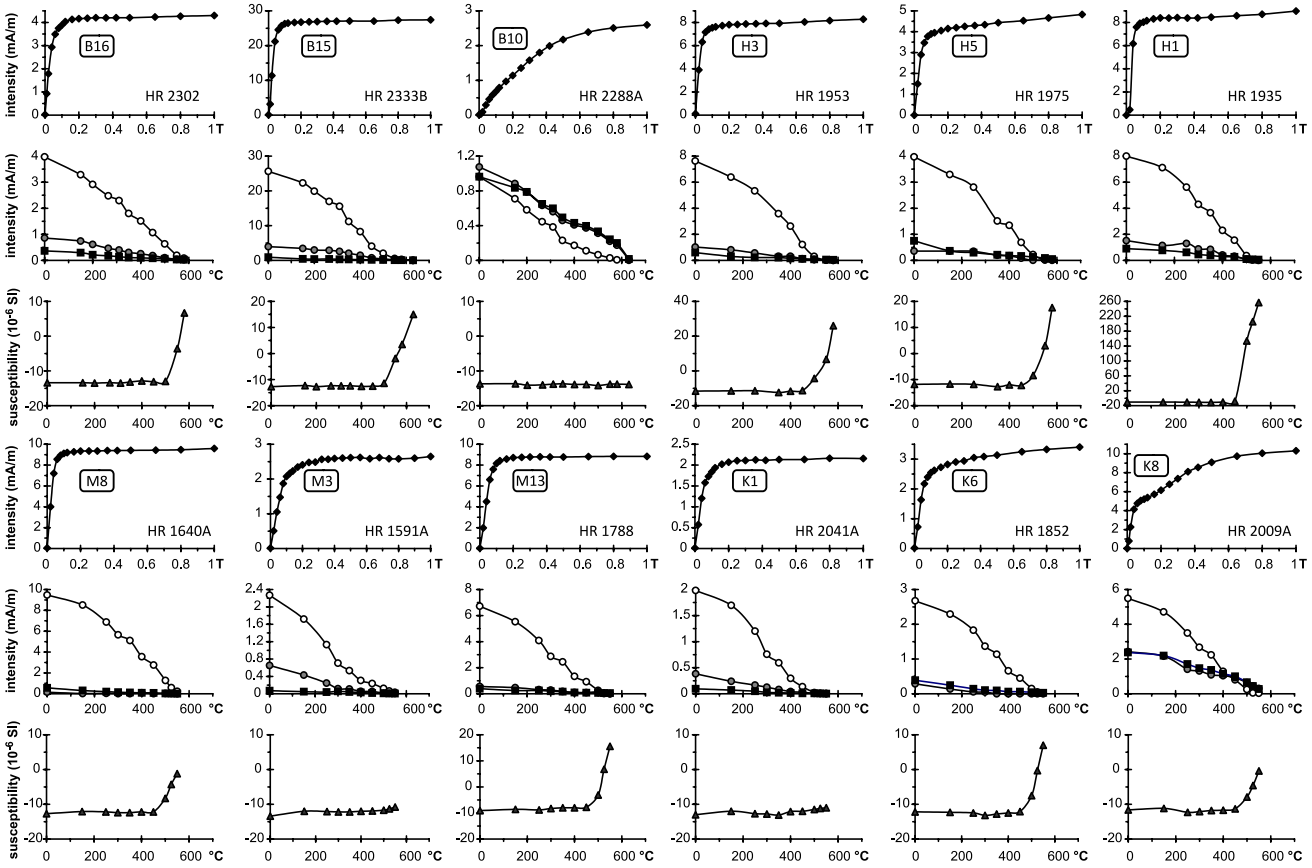

Fig. 7 Identification of the magnetic minerals (method by Lowrie, 1990) in Cretaceous platform limestones from Brač, Hvar, Mljet and Korčula islands.
From top to bottom: IRM acquisition, thermal demagnetization of the 3-component IRM, susceptibility after each demagnetization steps. The components of the IRM were acquired in fields of 1.0 T (squares), 0.36 T (full circles) and 0.12 T (open circles).

Fig. 8

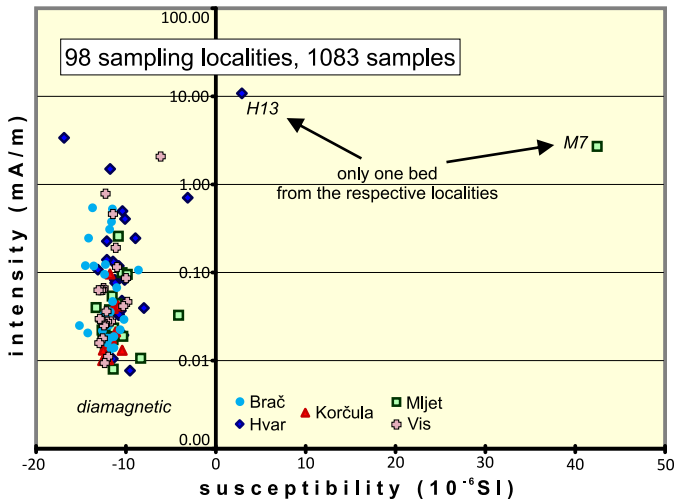

Fig. 8 Upper Jurassic through Lower Eocene carbonates of the NE Adriatic Carbonate Platform. Magnetic susceptibility vs. NRM intensity diagram based on locality mean values for the Central and Southern Adriatic islands.

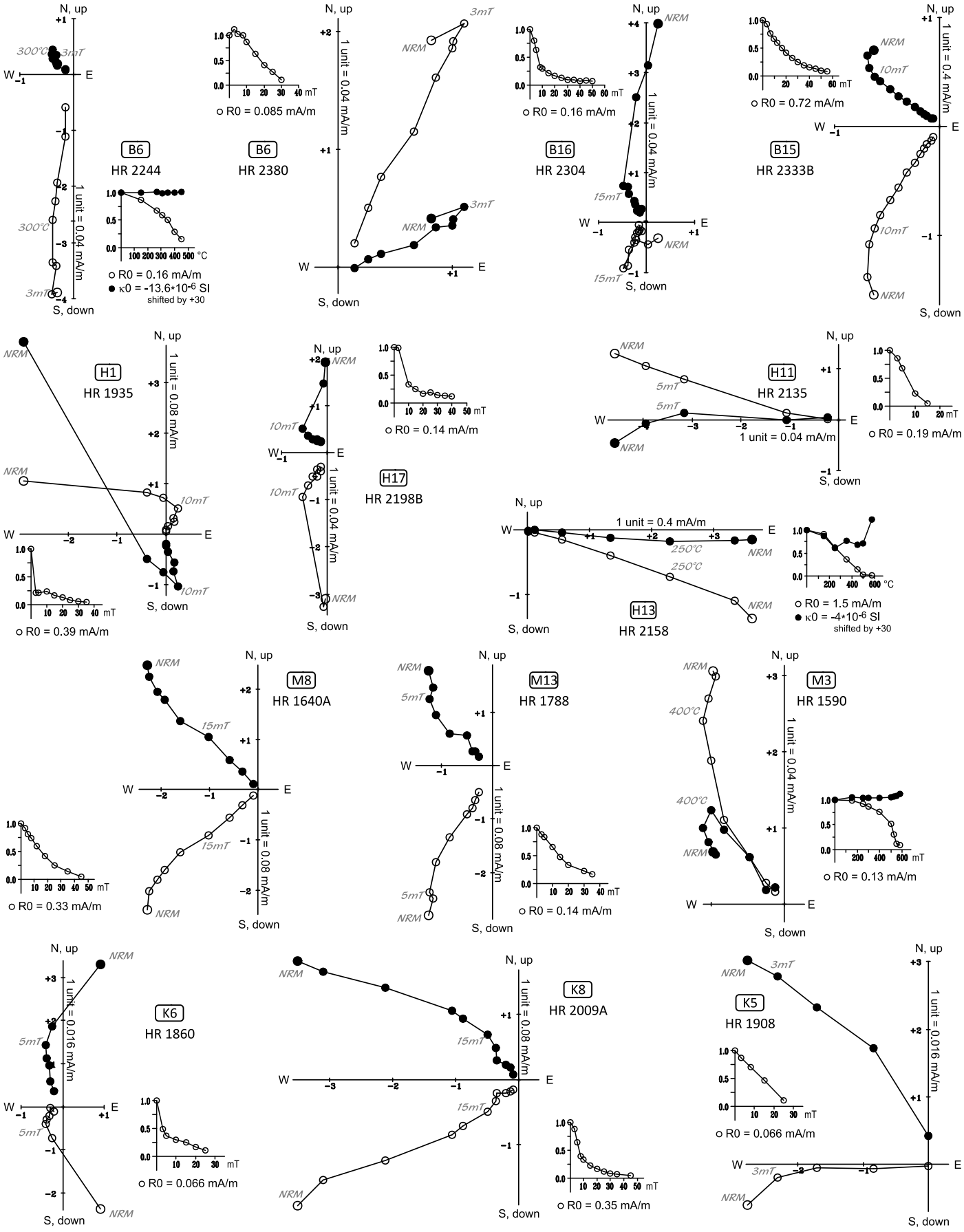

Fig. 9 Typical demagnetization curves for platform limestones of Brač, Hvar, Korčula and Mljet islands. Key: Zijderveld diagrams (Zijderveld, 1967) in geographic system. In case of AF demagnetization they are accompanied by intensity (circles) versus demagnetizing field diagrams, and by NRM intensity (circles)/susceptibility (dots) v.s. temperature diagrams, when the method is thermal (TH) demagnetization. In the Zijderveld diagrams full dots are the projections of the NRM vector onto the horizontal; circles: into the vertical.

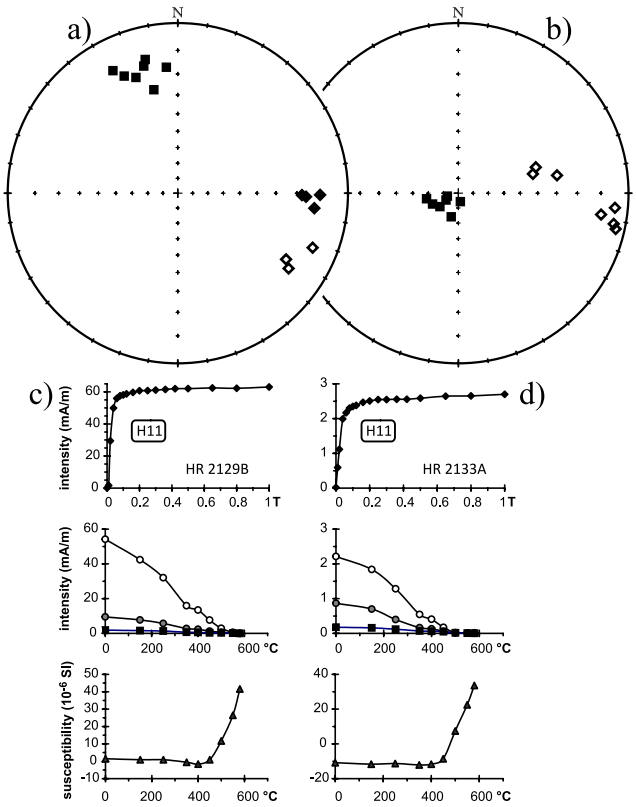

Fig. 10 Gromin Dolac (locality H11): ChRM directions from thin (squares) the thick (diamonds) beds before (a) and after (b) tilt correction. Stereographic projection, full symbols: positive, empty symbols: negative inclinations. c and d are the results of magnetic mineralogical experiments on samples with widely different NRM intensities. The ChRMs of the thin beds are probably the resultants of a CCW rotated remanence overprinted during a reversed polarity Chron, post-dating the CCW rotation (see the ChRMs of relatively close localities: K4 and H12), and eventually overprinted in the present Earth magnetic field. The ChRMs of the thick beds (over one meter) must be the resultants of a normal and reversed polarity remanence. For key see Fig.7).

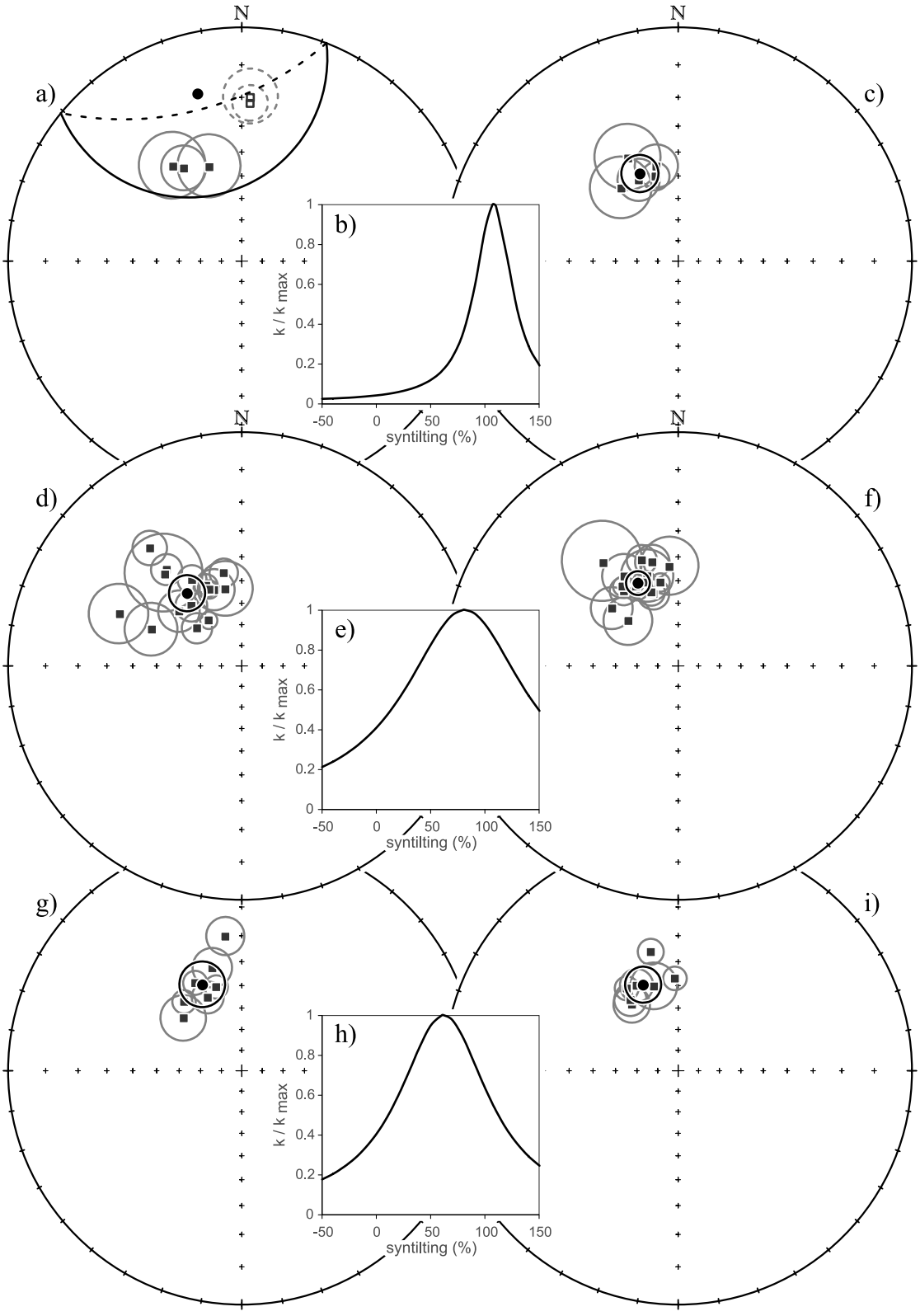

Fig. 11 Fold/tilt tests for the Northern Adriatic Islands Paleomagnetic locality mean directions (squares) and the overall-mean direction (dot) with α_{95} on stereographic plots ((positive inclinations:full,, negative inclination:empty symbols) before (left) and after (right) tilt corrections, accompanied by the results of the tilt test (in the middle) for the Turonian-Santonian (11 a-c), for the Albian-Cenomanian (11 d-f) and for the Barremian-Aptian (11 g-i).

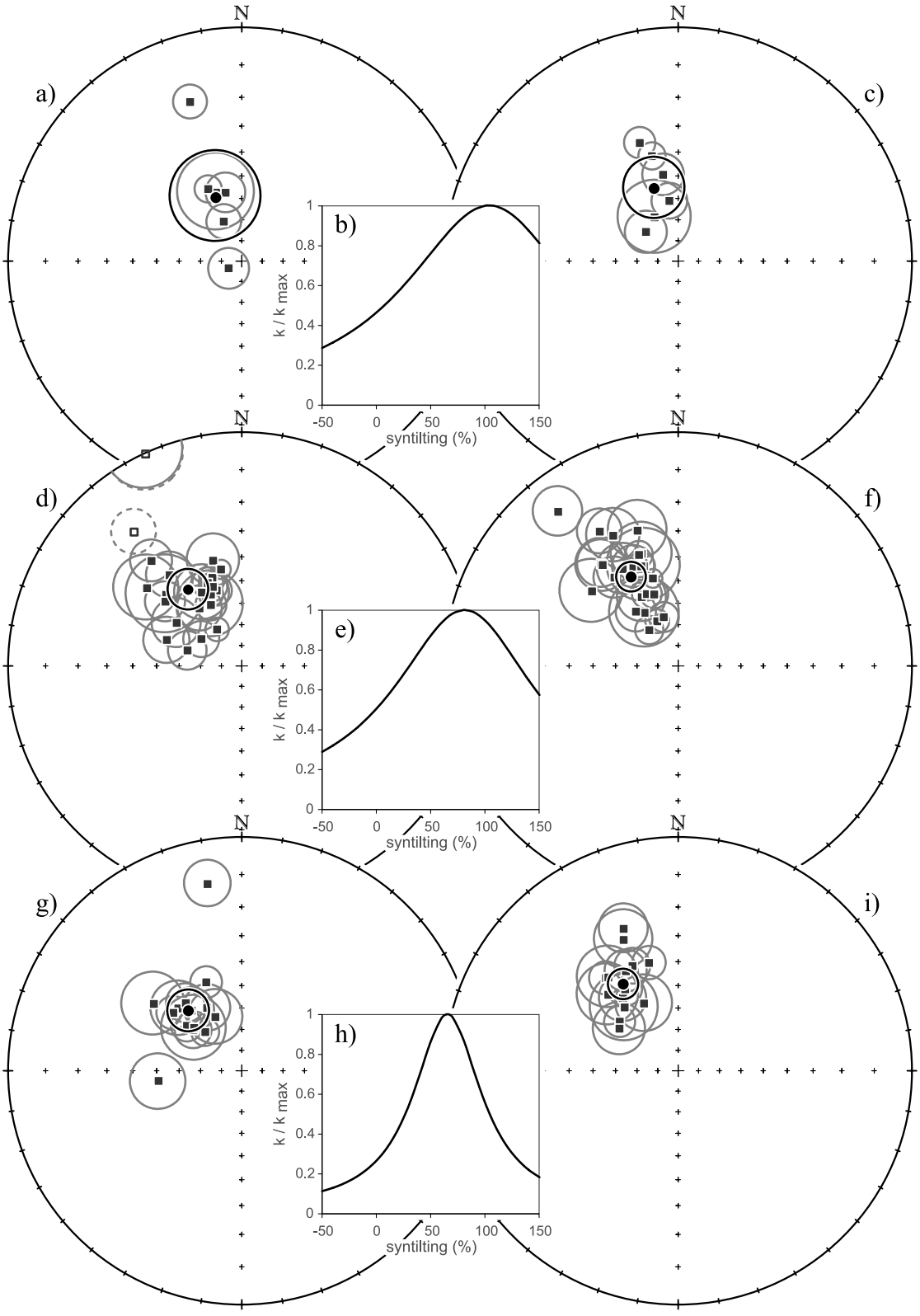

Fig. 12 Fold/tilt tests for the Central and Southern Adriatic islands. Paleomagnetic locality mean directions (squares) and the overall-mean direction (dot) with α_{95} on stereographic plots (positive inclinations:full,, negative inclination:empty symbols) before (left) and after (right) tilt corrections, accompanied by the results of the tilt test (in the middle) for the Campanian-Maastrichtian (12 a-c) , for the Turonian-Santonian (12 d-f) and the Albian-Cenomanian (12 g-i) carbonates. The test is indeterminate for the first and third age groups which were affected by well-documented syn-sedimentary tectonics during the Late Cenomanian and the Maastrichtian, respectively, while the deposition of the Turonian-Santonian carbonates took place during a tectonically quiet period (Prtoljan et al., 2007).

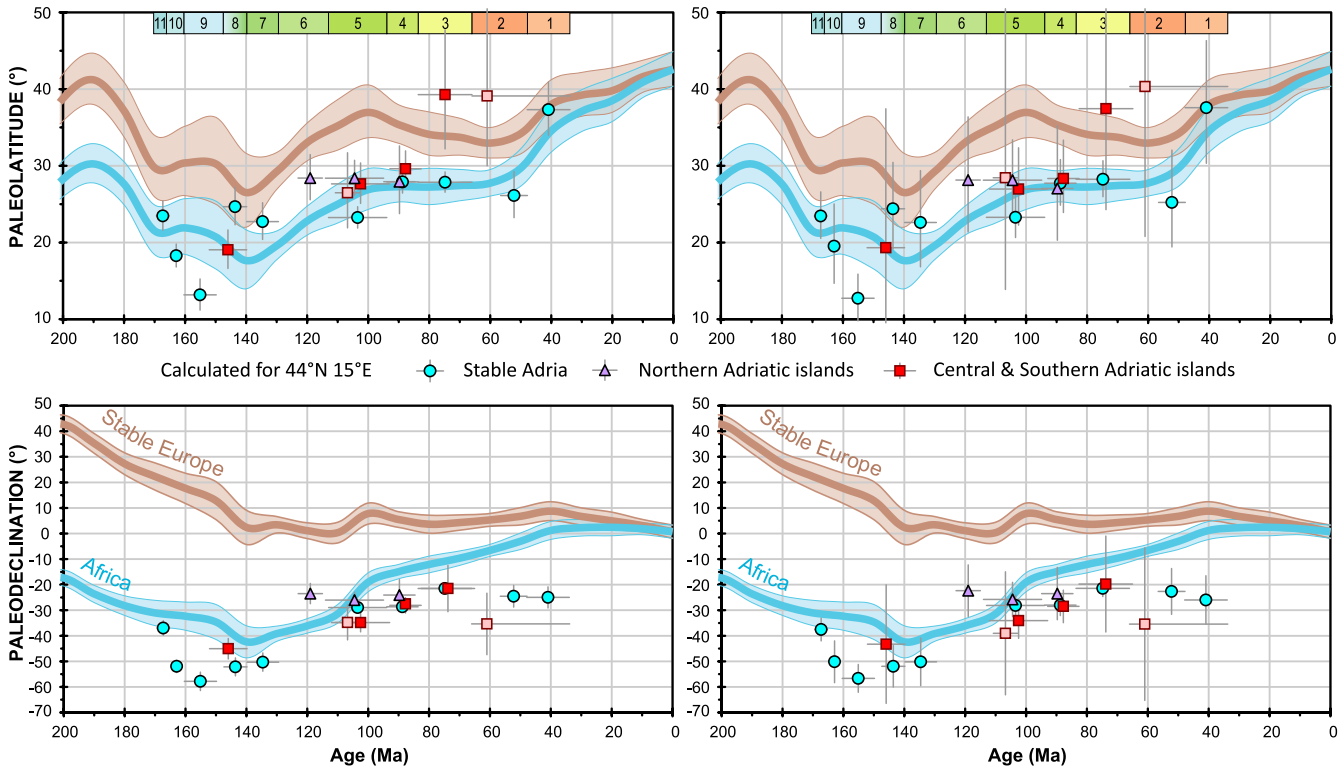

Fig. 13 Paleolatitudes and paleodeclinations for the NE part of the Adriatic region (stable Adria, Márton et al., 2017, Northen Adriatic islands, Márton et al., 2014, Central and southern Adriatic islands, present study) compared with those expected for stable Europe and Africa (Global APWP, Torsvik et al., 2012), respectively. The error bars for the paleomagnetic results are based on number of independently oriented samples (left side) and alternatively on the number of localities (right side). The error bars were computed based on Butler (1992). The geological age groups in the coloured bar are 1 = Priabonian – Lutetian, 2 = Paleocene – Ypresian, 3 = Campanian–Maastrichtian, 4 = Turonian–Santonian, 5 = Albian–Cenomanian, 6 = Barremian–Aptian, 7 = Valanginian–Hauterivian, 8 = Tithonian–Berriasian, 9 = Oxfordian–Tithonian, 10 = Callovian–Oxfordian, 11 = Bajocian-Bathonian. Lighter squares represent magnetization of post tilting age.

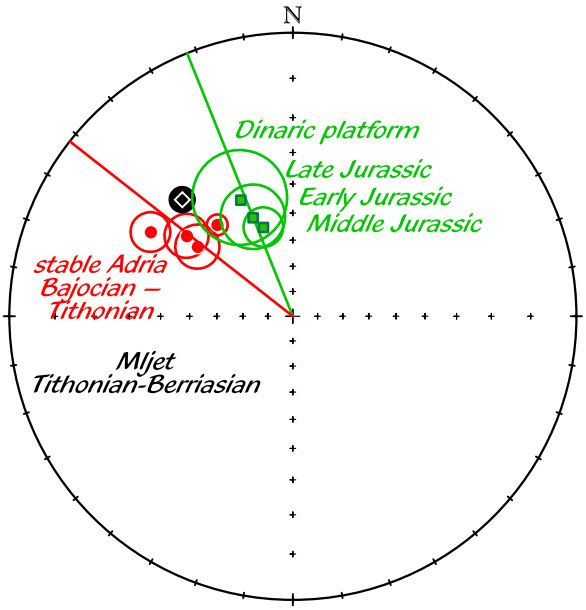

Fig. 14 Comparison of paleomagnetic overall-mean directions for Middle Jurassic-Earliest Cretaceous for stable Adria and for Mljet island, on one hand, and for rocks of similar ages from the High Karst between Rijeka and Zadar (stereographic plot, lower hemisphere).

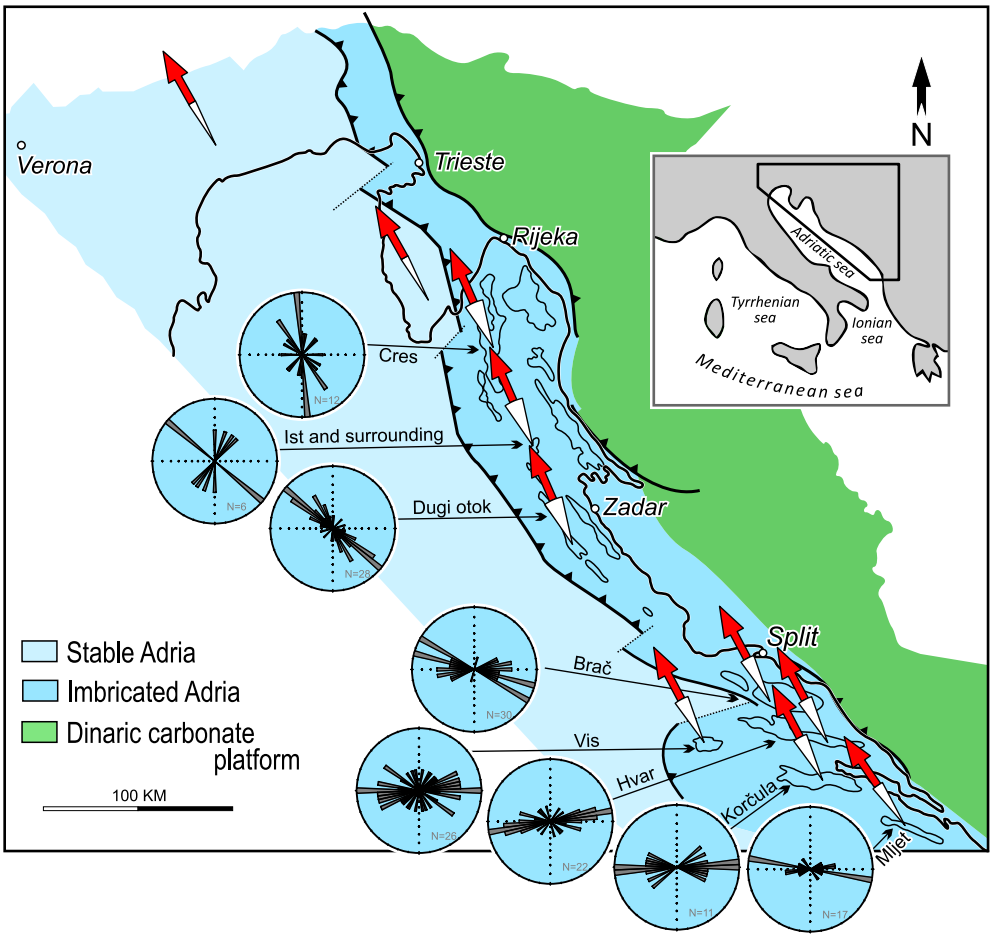

Fig. 15 The general tectonic subdivision of the NE part of the Adriatic region after Tari (2002) with Turonian-Santonian paleomagnetic declinations (arrows with statistical errors) illustrate the lack of relative movements between the islands and with respect to stable Adria, which is proved by all paleomagnetic data after the Late Aptian-Early Albian tectonic event. The arcuate shape of imbricated Adria is explained by the dominance of one of the three main compressional regime of different orientations, getting younger from NW to SE (Marinčić, 1997). The rose diagrams based on our strike measurements in the field are presented to show that the tectonic strikes reflect in Cres island the dominance of the uppermost Cretaceous Laramian (N-S), in Ist and Dugi Otok islands the mid-Eocene-Oligocene (NW-SE) and (in the Central and Southern Adriatic the neotectonic phase (WNW-ESE) tectonic structures.

Table 1. Brač, Mljet, Korčula, Hvar and Vis islands. Summary of locality mean palaeomagnetic directions based on the results of principal component analysis (Kirschvink 1980), except localities B17, H5, H10 and V23, where combination of stable end points and demagnetization circles was used (McFadden and McElhinny 1988).
Key: Lat.N, Lon.E: Geographic coordinates (WGS84) measured by GPS, n/no: number of used/collected samples (the samples are independently oriented cores); D, I (Dc, Ic): declination, inclination before (after) tilt correction; k and α95: statistical parameters (Fisher 1953); Paleo lat: paleolatitude; Pole lat and Pole long: coordinates of the paleopole; δm, δp: statistical parameters of the palaeomagnetic pole. *: post-tilting magnetization, pole calculated from directions before tilt correction; **: rejected from tectonic interpretation, very young remagnetization, poles not calculated.

		Locality	Age	Lat (˚) Lon (˚)	n/no	D (˚)	I (˚)	k	α_{95}(˚)	Dc (˚)	Ic (˚)	k	α_{95}(˚)	Dip	Paleo lat (˚)	Pole lat (˚)	Pole long (˚)	dp (˚)	dm (˚)
		Brač																	
1	B17	Milna, Maslinova HR2247-258	Cenomanian - Turonian	43°18'28" 16°27'58"	7/12	341.6	+46.7	123.6	5.6	334.8	+66.3	123.6	5.6	171/20	48.7	71.8	312.5	7.5	9.2
2	B16	Bol, Sveti Duh HR2294-304	Lower Turonian	43°16'02" 16°42'00"	6/11	313.2	+42.2	18.8	15.8	327.7	+59.9	18.8	15.8	107/21	40.8	66.0	291.9	18.0	23.9
3	B15	Vidova Gora HR2328-335, 2423-441	Turonian	43°16'59" 16°37'14"	7/8	310.1	+43.8	53.8	8.3	324.2	+40.1	53.8	8.3	32/16, 16/10, 338/14, 1/35	22.8	54.1	263.5	6.0	10.0
4	B11	Hunćac ** HR2316-327	Upper Turonian - Lower Campanian	43°18'19" 16°32'16"	5/14	8.2	+59.4	112.0	7.3	8.2	+59.4	112.0	7.3	360/0					
5	B8	Pučišča SLO1930-942	Upper Turonian - Lower Campanian	43°21'32" 16°44'39"	4/13	331.5	+50.7	61.9	11.8	341.9	+36.5	60.9	11.9	340/18, 9/18, 24/15	20.3	62.4	235.7	8.1	13.8
6	B12	Vela Grška HR2350-362	Coniacian - Campanian	43°17'22" 16°28'59"	9/13	341.6	+52.5	60.6	6.7	321.1	+67.8	60.6	6.7	189/19	50.8	62.8	316.2	9.3	11.1
7	B10	Planica HR2282-293	Coniacian - Campanian	43°16'16" 16°32'52"	6/12	321.2	-17.4	88.9	7.1	322.1	+10.3	88.9	7.1	169/31	5.2	39.4	248.9	3.7	7.2
8	B6	Nerežišče HR2235-246, 2376-399	Campanian	43°19'54" 16°35'54"	12/36	241.3	+82.7	20.0	10.0	312.2	+68.9	20.0	10.0	333/20	52.3	57.3	319.6	14.3	16.9
9	B1a	Sutivan-Borak * SLO1317-320	Campanian - Maastrichtian	43°23'19" 16°27'37"	4/4	116.8	-43.9	322.3	5.1	128.4	-28.3	322.3	5.1	348/22	25.7	36.4	289.0	4.0	6.4
10	B2	Postire SLO1726-731	Maastrichtian	43°22'20" 16°37'07"	5/6	346.6	+56.6	74.9	8.9	350.1	+49.0	74.9	8.9	8/8	29.9	74.4	230.3	7.8	11.8
11	B3	Mirca SLO1755-762	Maastrichtian	43°22'56" 16°29'03"	6/8	335.5	+69	67.3	8.2	351.7	+60.9	67.3	8.2	27/11	41.9	83.7	276.0	9.6	12.6
12	B4	Sumartin SLO1321-326	Maastrichtian	43°17'08" 16°52'09"	4/6	339.4	+55.3	30.2	17.0	331.8	+66.6	30.2	17.0	176/12	49.1	69.8	313.5	23.1	28.0

13	B5	Splitska SLO1327-334	Maastrichtian	43°22'56" 16°36'09"	8/8	154.9	-52.5	86.9	6.0	162.5	-34.1	86.9	6.0	2/20	18.7	61.3	232.9	3.9	6.8
14	B1b	Sutivan-Borak * SLO1270-273	Paleocene	43°23'18" 16°27'35"	4/4	159.0	-52.7	168.7	7.1	172.8	-38.9	168.7	7.1	30/19	33.3	70.8	261.8	6.7	9.8
15	B1c	Sutivan-Borak * SLO1748-752	Paleocene	43°23'22" 16°27'34"	5/5	330.0	+58.0	35.3	13.1	322.0	+48.0	35.3	13.1	14/18	38.7	67.0	284.9	14.2	19.2
16	B1d	Sutivan-Borak * SLO1282-287	Paleocene	43°23'23" 16°27'30"	3/6	322.1	+79.0	99.9	12.4	353.8	+65.9	99.9	12.4	16/16	68.8	58.0	351.6	22.4	23.5
17	B1e	Sutivan-Borak * SLO1288-293	Paleocene	43°23'22" 16°27'28"	4/6	156.9	-43.2	161.6	7.3	157.2	-35.2	161.6	7.3	340/8	25.2	63.8	249.9	5.6	9.0
		Mljet																	
18	M14	Sutmiholjska HR1835-846	Tithonian	42°44'08" 17°30'29"	9/12	333.4	+45.7	36.6	8.6	334.2	+32.7	36.6	8.6	338/13	17.8	56.8	246.7	5.5	9.7
19	M8	Vrata Solina HR1640-651, 1721-730	Upper Tithonian - Lower Valanginian	42°46'03" 17°23'17"	18/22	311.1	+34.9	216.8	2.4	315.3	+27.6	216.8	2.4	357/10	14.6	42.6	264.9	1.4	2.6
20	M11	Punta Križa HR1731-742	Upper Tithonian - Lower Valanginian	42°45'59" 17°23'14"	12/12	297.7	+42.3	58.2	5.7	305.1	+33.3	58.2	5.7	348/13	18.2	37.8	277.0	3.7	6.5
21	M3	Okuklja Bay * HR1590-601, 1707-718	Lower Barremian	42°43'57" 17°40'10"	19/24	329.5	+47.7	17.7	8.2	342.0	+16.8	17.7	8.2	8/36	28.8	61.8	268.0	7.0	10.7
22	M1	Maranoviči HR1568-579, 1699-706	Albian	42°43'24" 17°40'08"	11/20	310.1	+59.7	30.5	8.4	339.3	+24.6	30.5	8.4	7/45	12.9	55.2	234.8	4.8	9.0
23	M13	Lokve bay HR1788-797	Albian	42°47'02" 17°19'58"	7/12	316.7	+64.4	88.0	6.5	322.0	+36.7	88.0	6.5	328/28	20.4	51.2	264.3	4.4	7.6
24	M7	Paselo * HR1630-639, 1743-757, 1798-812	Upper Albian - Middle Cenomanian	42°44'02" 17°38'08"	10/40	303.0	+38.7	28.4	9.2	318.0	+11.0	28.4	9.2	1/41	21.8	38.6	282.5	6.5	11.0
25	M12	Kozarica HR1758-767	Cenomanian	42°46'39" 17°26'60"	13/26	263.0	+50.6	12.9	12.0	323.2	+37.1	12.9	12.0	12/56	20.7	52.2	263.5	8.3	14.1
		Korčula																	
26	K5	Grščica * HR1895-908	Barremian - Albian	42°54'33" 16°44'54"	14/14	333.7	+18.1	30.0	7.4	304.5	+47.6	30.0	7.4	196/50	9.3	49.3	238.8	4.0	7.7

27	K6	Karbuni-1 HR1847-865	Albian	42°55'17" 16°43'23"	18/18	349.6	+11.9	26.3	6.9	308.9	+53.5	26.3	6.9	206/66	34.0	49.7	291.7	6.7	9.6
28	K10	Babina HR2021-030	Albian	42°57'35" 16°56'59"	4/10	331.1	+55.9	78.6	10.4	337.4	+27.6	78.6	10.4	348/29	14.6	55.7	238.2	6.2	11.4
29	K8	Zavalatica HR1999-2009	Cenomanian - Turonian	42°55'02" 16°56'04"	6/11	321.5	+37.3	55.6	9.1	322.2	+57.3	55.6	9.1	140/20	37.9	61.0	290.0	9.7	13.2
30	K4	Blaca ** HR1866-878	Turonian	42°57'26" 16°51'21"	5/13	180.5	-57.5	52.2	10.7	182.6	-23.6	52.2	10.7	6/34					
31	K9	Blaca HR2010-020	Turonian	42°57'26" 16°51'21"	10/11	303.6	+66.6	33.5	8.5	335.7	+40.1	33.5	8.5	2/34	22.8	61.5	249.6	6.1	10.2
32	K1	Račišče, Samograd bay HR1879-894, 2041-	Coniacian - Santonian	42°58'27" 16°59'36"	8/21	106.5	-62.9	39.4	8.9	143.3	-32.7	39.4	8.9	353/42	17.8	50.1	259.4	5.7	10.1
		Hvar																	
33	H19	Pitve * HR2209-215	Neocomian	43°08'37" 16°40'23"	6/7	297.9	+56.1	31.4	12.1	209.4	+44.1	31.4	12.1	171/61	36.7	43.0	300.8	12.6	17.5
34	H13	Križišče HR2153-162	Upper Albian	43°08'34" 16°47'18"	7/10	314.5	+48.4	27.9	11.6	305.7	+55.7	27.9	11.6	173/10	36.2	48.4	296.3	11.9	16.6
35	H7	Maslinica bay, Vrbovska HR2079-094	Cenomanian	43°11'22" 16°40'22"	14/16	309.3	+56.3	32.5	7.1	336.4	+38	32.5	7.1	17/30	21.3	60.6	246.1	4.9	8.4
36	H15	Basina HR2175-184	Cenomanian	43°11'51" 16°39'20"	9/10	320.4	+48.9	38.7	8.4	332.3	+38.7	38.7	8.4	17/16	21.8	58.6	252.6	5.9	10.0
37	H3	Poljica, Stiniva bay HR1952-961	Cenomanian	43°09'30" 16°47'11"	9/10	320.2	+53	27.7	10.0	322.8	+47.4	27.7	10.0	343/6	28.5	56.8	273.0	8.4	13.0
38	H4	Poljica HR1962-967	(Cenomanian-) Turonian	43°09'30" 16°46'59"	5/6	319.3	+28.8	101.3	7.6	329.7	+22.8	101.3	7.6	39/22	11.9	49.2	245.9	4.3	8.1
39	H5	Nova Crkva HR1968-976, 2204-208	Turonian - Santonian	43°07'30" 16°56'35"	7/14	335.6	-0.3	47.9	9.4	333.5	+26.3	47.9	9.4	173/28	13.9	52.9	242.9	5.5	10.2
40	H14	Rudine HR2163-174	Turonian - Santonian	43°11'41" 16°35'55"	8/12	344.8	+40	28.8	10.5	343.3	+27.8	24.8	11.3	359/8, 340/15, 303/15	14.8	58.2	228.4	6.8	12.4
41	H16	Zavala bay HR2185-193	Turonian - Santonian	43°08'48" 16°59'24"	9/9	289.1	+52.6	26.9	10.1	323.2	+33.4	26.9	10.1	9/39	18.2	50.3	259.9	6.5	11.5

42	H17	Bristova bay HR2194-203	Turonian - Santonian	43°08'27" 17°00'41"	9/10	303.5	+53.1	23.7	10.8	332.1	+53.2	23.7	10.8	48/21	33.8	66.4	273.0	10.4	15.0
43	H9	Vira 1 HR2106-114	Turonian - Santonian	43°11'21" 16°25'37"	8/9	336.7	+53.2	106.2	5.4	340.6	+36.7	106.2	5.4	352/17	20.4	62.1	238.0	3.7	6.3
44	H10	Vira 2 HR2115-125	Turonian - Santonian	43°11'23" 16°25'50"	6/11	323.7	+56.1	75.6	9.2	329.9	+40	75.6	9.2	346/17	22.8	57.8	256.7	6.7	11.1
45	H11	Gromin Dolac HR2126-133	Turonian - Santonian	43°07'36" 16°44'05"	8/8	344.9	+14.4	77.4	6.3	242.3	+80.6	77.4	6.3	174/79	71.7	32.8	357.4	11.7	12.1
46	H11	Gromin Dolac HR2134-139	Turonian - Santonian	43°07'36" 16°44'05"	5/6	273.3	-13.2	262.9	4.7	278.8	+6.4	262.9	4.7	174/79	3.2	8.6	283.0	2.4	4.7
47	H11	Gromin Dolac HR2140-142	Turonian - Santonian	43°07'36" 16°44'05"	3/4	299.2	+13.1	122.4	11.2	255.7	+36.4	122.4	11.2	174/79	20.2	3.9	311.1	7.6	13.1
48	H12	Uvala Soča ** HR2143-152	Turonian - Santonian	43°06'55" 16°56'38"	9/10	210.2	-41.7	13.6	14.5	312.2	-58.0	13.6	14.5	179/67					
49	H1	Perna HR1934-943	Campanian	43°07'24" 17°09'51"	6/10	162.1	-18.9	128.9	5.9	165.7	-40.4	146.4	5.6	144/22, 170/26	23.1	66.7	232.2	4.1	6.7
		Vis																	
50	V1	Titova Spilja * HR1524-538	Early Cretaceous	43°01'55" 16°07'22"	6/15	322.9	+48.8	48.4	9.7	324.2	+56.7	48.4	9.7	118/9, 154/8	29.7	57.6	274.3	8.5	12.8
51	V2	Mali Hum 1 HR1545-550	Albian	43°03'11" 16°06'58"	5/6	307.2	+39.5	38.3	12.5	317.4	+42.4	38.3	12.5	56/12	24.5	50.6	272.1	9.5	15.4
52	V3	Mali Hum 2 HR1562-567	Albian	43°03'02" 16°06'53"	5/6	310.2	+48.1	116.0	7.1	326.9	+44.85	116.0	7.1	37/16	26.4	58.4	265.2	5.7	9.0
53	V4	Sv. Mihovil YM1181-189	Aptian	43°02'54" 16°06'49"	8/8	301.0	+55	26.0	11.0	316.4	+49.1	26.0	11.0	78/10?	30.0	53.1	280.1	9.6	14.6
54	V7	Vis, Hotel Issa HR1500-511	Cenomanian	43°04'04" 16°11'18"	8/12	338.1	+45.7	70.2	6.7	344.9	+39	70.2	6.7	30/10	22.0	65.5	231.8	4.7	7.9
55	V9	Vis, Town HR877-886	Cenomanian	43°03'52" 16°12'14"	5/10	333.8	+61.3	38.5	12.5	333.1	+54.3	38.5	12.5	330/7	34.8	67.6	273.7	12.4	17.6
56	V11	Vis, Grandovac HR1482-487	Cenomanian	43°03'59" 16°12'17"	4/6	311.9	+59.4	40.1	14.7	319.8	+51	40.1	14.7	349/10	31.7	56.5	280.0	13.4	19.9

57	V12	Rogačića HR917-926	Turonian – Lower Santonian	43°04'33" 16°10'55"	3/10	332.9	+57.1	70.8	14.8	341.0	+41.5	70.8	14.8	1/17	23.9	65.2	241.4	11.0	18.0
58	V13	Parja YM1946-955	Turonian – Lower Santonian	43°04'43" 16°10'42"	9/10	325.9	+68.7	112.9	4.9	339.7	+41.16	86.2	5.6	352/25	23.6	64.3	243.3	4.1	6.8
59	V16	Oključna ** YM1898-906	Turonian – Lower Santonian	43°04'26" 16°07'22"	8/9	7.0	+69	173.0	4.0	7.0	+30	173.0	4.0	10/38					
60	V18	Rukavac ** YM1925-933	Turonian – Lower Santonian	43°01'17" 16°12'43"	8/9	13.0	+53	33.0	10.0	16.0	+64	33.0	10.0	175/5					
61	V19	Rukavac HR859-866	Turonian – Lower Santonian	43°01'17" 16°12'43"	8/8	337.7	+48.1	72.2	6.6	336.5	+53.0	72.2	6.6	165/5	33.6	69.4	266.8	6.3	9.1
62	V20	Srebrna YM1934-945	Turonian – Lower Santonian	43°01'15" 16°12'19"	12/12	347.9	+44.3	117.7	4.0	343.9	+47.5	117.7	4.0	216/5	28.6	70.6	243.4	3.4	5.2
63	V21	Srebrna HR867-876	Turonian – Lower Santonian	43°01'15" 16°12'19"	7/10	339.9	+50.5	95.1	6.2	341.5	+54.3	95.1	6.2	143/4	34.8	73.5	262.7	6.2	8.7
64	V22	Srebrna bay HR939-952	Turonian – Lower Santonian	43°01'07" 16°12'16"	7/14	309.4	+34.7	24.6	12.4	310.9	+38.1	24.6	12.4	99/4	21.4	44.0	274.2	8.7	14.7
65	V23	Termule HR1488-499	Turonian – Lower Santonian	43°01'06" 16°11'29"	10/12	333.2	+57.5	56.3	6.9	343.1	+65.96	56.3	6.9	126/10	48.3	77.1	316.0	9.1	11.2

Table 2.

	PALEOMAGNETIC DIRECTION									FOLD/TILT TEST; REVERSAL TEST	PALEOMAGNETIC POLE								
											Based on localities				Based on samples				
	N	D°	I°	k	α_{95}°	D_C°	I_C°	k	α_{95}°	Optimal untilting and classification; classification of reversal test	Lat.	Long.	K	A95	n	Lat.	Long.	K	A95
Northern islands: Cres, Ist & surrounding, Dugi Otok																			
Turonian – Santonian (C, I&, DO)	5	345.2	17.1	4.7	39.8	**336.4**	**45.8**	97.0	7.8	107 ± 28, positive	64.6	250.9	71.8	9.1	29	64.9	253.2	26.4	5.3
Albian – Cenomanian (C, I&, DO)	15	323.0	47.7	25.7	7.7	**334.1**	**47.1**	58.1	5.1	83 ± 26, positive	64.0	256.0	43.9	5.8	126	64.0	256.8	22.5	2.7
Barremian – Aptian (DO)	7	335.4	46.1	40.5	9.6	**337.8**	**46.9**	63.4	7.6	62 ± 49, positive	66.1	250.9	47.0	8.9	75	65.6	253.1	22.6	3.5
Southern islands: Brač, Mljet, Korčula, Hvar, Vis																			
Paleocene (B)	5	**324.8**	**56.4**	20.4	17.4	332.6	44.6	16.2	19.6	-9 ± 199, indeterminate; Ro	63.7	289.4	12.8	22.2	20	63.3	286.7	13.3	9.3
Campanian – Maastrichtian (B, H)	6	337.8	57.4	11.9	20.2	**341.7**	**53.9**	25.4	13.6	103 ± 113, indeterminate; Ro	73.7	268.5	21.1	14.9	41	73.3	276.0	11.1	7.0
Turonian – Santonian (B, K, H, V)	23	324.9	46.6	13.4	8.6	**332.1**	**43.5**	25.2	6.1	82 ± 27, positive	62.4	260.1	30.5	5.6	171	63.5	261.6	18.5	2.6
Albian – Cenomanian (M, K, H, V)	14	318.3	52.2	19.9	9.1	**327.5**	**42.7**	41.6	6.2	66 ± 17, indeterminate	57.8	264.5	42.5	6.2	119	57.7	266.2	17.1	3.2
Barremian-Aptian	4	**323.3**	**43.6**	16.6	23.3	306.1	53.6	3.7	56.1	0 ± 138, indeterminate	55.3	271.6	20.2	21.0	45	57.0	264.6	13.3	6.1
Tithonian-Berriasian	3	313.6	41.9	32.4	22.0	**318.1**	**31.8**	39.8	19.8	indeterminate	46.3	264.8	32.8	21.9	39	45.0	266.1	37.4	3.8
Stable Adria: Istria, Adige embayment																			
Priabonian – Lutetian	8	334.5	55.7	74.5	6.5	**333.4**	**58.2**	75.4	6.4	51 ± 92, indeterminate; Rb	69.4	275.8	55.9	7.5	71	70.0	274.1	26.6	3.3
(Paleocene) – Ypresian	11	335.4	43.3	30.7	8.4	**336.1**	**45.1**	37.6	7.5	85 ± 87, indeterminate; Rb	63.7	246.9	32.9	8.1	77	63.3	251.1	18.7	3.8
Campanian–Maastrichtian *	7	339.3	38.8	51.1	8.5	**337.2**	**49.4**	472.5	2.8	111 ± 32, positive; Ra	66.7	249.6	482.3	2.8	42	66.4	249.0	179.8	1.6
Turonian–Santonian *	21	327.9	37.4	42.5	4.9	**330.7**	**48.5**	108.5	3.1	104 ± 38, positive	62.3	258.4	77.3	3.6	196	62.0	259.5	33.3	1.8
Albian–Cenomanian *	15	328.5	37.6	32.1	6.9	**330.6**	**43.0**	131.1	3.4	93 ± 27, positive	59.0	252.3	108.9	3.7	136	58.5	253.3	40.2	1.9
Valanginian–Hauterivian	7	306.8	42.0	64.6	7.6	**308.0**	**42.9**	66.8	7.4	52 ± 45, indeterminate; Rc	43.8	274.3	50.1	8.6	63	43.8	274.5	31.2	3.3
Tithonian–Berriasian	4	307.2	41.4	69.6	11.1	**306.1**	**45.0**	148.9	7.6	111 ± 239, indeterminate; Rb	43.7	277.6	157.1	7.4	34	43.7	278.1	58.4	3.2
Oxfordian-Tithonian	4	301.7	29.5	121.8	8.4	**300.6**	**29.7**	233.6	6.0	67 ± 125 indeterminate; Rb	32.6	270.3	296.0	5.3	30	32.1	271.6	58.4	3.5
Callovian-Oxfordian	4	308.6	38.7	92.1	9.6	**307.1**	**39.9**	161.5	7.3	89 ± 106 indeterminate	41.8	271.1	142.0	7.7	217	39.7	271.4	14.1	2.7
Bajocian-Bathonian	9	325.2	44.0	94.2	5.3	**320.4**	**44.7**	206.1	3.6	115 ± 50 positive; Ra	53.1	263.6	161.1	4.1	64	53.5	263.0	48.9	2.6

Table 2. Summary of the overall mean paleomagnetic directions before and after tilt corrections, results of direction correction tilt test (Enkin, 2008) and reversal test (McFadden and McElhinney, 1990) and paleomagnetic poles with statistical parameters. Key as for Table 1. but N is the number of localities. * E/I

corrected (Tauxe and Kent, 2004). Callovian-Oxfordian date are from Channell et al., 1990, 2010, Muttoni et al., 2013. K was calculated based on the method by Cox (1970) for Callovian-Oxfordian pole based on samples.

Supplementary Table 1. Description of localities and samples

No in tables and maps	Localities	Texture (after Dunham, 1962; Embry & Klovan, 1972) and Flügel (2010)	Fossil content	Age attribution after Geological map of former YU	Accepted ages for this study [revised after Geological map of Croatia (2010*, **) and our findings]
B18	Zagvozd	(1) Laminated wackestones (2) Grainstones	(1) Ostracods, *Thaumatoporella parvovesiculifera* (Raineri), *Decastronema kotori* (Radoičić) [confided to one layer] (2) *Thaumatoporella parvovesiculifera* (Raineri), miliolids, *Nummmuloculina* (*Pseudonummuloculina*) *heimi* Bonet	Coniacian	CENOMANIAN - CONIACIAN
B6	Nerežišča (quarry)	Wackestones	Planktonic foraminifera: *Hedbergella planispira* (Tappan), *Globotruncana rosetta* (Carsey)	Campanian	CAMPANIAN
B17	Maslinova Milna (bay)	Laminated microbial bindstones	*Thaumatoporella parvovesiculifera* (Raineri), irregular globose morphotypes, undeterminable miliolids (*Istriloculina* sp.), rare fragments of bivalves	Cenomanian – Turonian	CENOMANIAN-
B1	Sutivan – Likva bay	2018: Grainstones 2017a: Packstones 2017: Laminated biomicral bindstones, 2017 Borak: Packstones – grainstones	2018: Charae, miliolids (undeterminable), *Hottingerina lukasi* Drobne, *Lockhartia* sp. 2017a: fragments of bivalves, echinoids, miliolids, textulariids and indeterminant rotaliids *Coskinolina liburnica* Stache, *Lithoporella melobesioides* (Foslie) 2017: *Thaumatoporella parvovesiculifera* (Raineri) 2017 Borak*: Idalina* sp., *Orbitolites* sp., small miliolids and rotaliids, *Spirolina* sp., *Chrysalidina* sp., *Solenomeris* (*Gypsina* sp,) sp.	Late Cretaceous Eocene	2018: THANETIAN (Paleocene) 2017: YPRESIAN (SBZ 11 – 12),
B8	Pučišća (quarry)	Dolomitized wackestones – packstones	Fragments of bivalves	Upper Turonian – Lower Campanian	UPPER TURONIAN - CAMPANIAN
B3	Mirca	Dolomites		Maastrichtian	MAASTRICHTIAN
B16	Bol, Sv. Duh	Mudstones – wackestones	Ostracods, rare *Girvanella* filaments, undeterminable rotaliids	Lower Turonian	LOWER TURONIAN
B9	Gračišće	Packstones – grainstones	*Thaumatoporella parvovesiculifera* (Raineri), *Decastonema kotori* (Radoičić), *Moncharmontia apenninica* (De Castro), undeterminable miliolids	Upper Turonian - Lower Campanian	UPPER TURONIAN – LOWER CAMPANIAN
B10	Planica	Packstones, rare dolomite grains	*Thaumatoporella parvovesiculifera* (Raineri), undeterminable agglutinated benthic foraminifera and miliolids, *Moncharmontia apenninica* (De Castro),	Upper Turonian - Lower Campanian	CAMPANIAN (CONIACIAN – CAMPANIAN[1])

			Accordiella conica (Farinacci), *Scandonea* sp., *Rotalispira* sp., *Pilatorotalia* sp.		
B11	Hunčac	*Decastronema* wackestones	*Decastronema kotori* (Radoičić), underminable miliolids (*Istriloculina* sp.)	Upper Turonian - Lower Campanian	LOWER TURONIN - CAMPANIAN
B12	Grška bay	Wackestones – packstones	*Moncharmontia apenninica* (De Castro), *Decastonema kotori* (Radoičić), *Thaumatoporella parvovesiculifera* (Raineri), *Scandonea* sp., undeterminable miliolids, ostracods	Upper Turonian – Lower Campanian	UPPER TURONIAN – LOWER CAMPANIAN (CONIACIAN – CAMPANIAN[1])
B13	Grižev promontory	Wackestones, rare dolomite grains	*Rotalispira vitigliana* Consorti, Frijia & Caus, *Stensioeina surrentina* Torre, *Decastronema kotori* (Radoičić), *Thaumatoporella parvovesiculifera* (Raineri), *Murgella* sp., *Scandonea* sp., undeterminable agglutinated foraminifera (*Bolivinopsis* sp.?), ostracods	Upper Turonian – Lower Campanian	CAMPANIAN[2]
B14	Milna, olive grove	*Decastronema* wackestones – packstones	*Decastronema kotori* (Radoičić), *Thaumatoporella parvovesiculifera* (Raineri), *Moncharmontia apenninica* (De Castro), *Girvanella* filaments, *Valvulamina* sp., Fragments of bivalves	Upper Turonian - Campanian	CAMPANIAN (CONIACIAN-CAMPANIAN[1])
B15	Vidova gora	Laminated microbial bindstones	*Thaumatoporella parvovesiculifera* (Raineri), Nubeculariid foraminifera, undeterminble miliolids	Turonian	TURONIAN
B7	Road to Pučišća quarry	Wackestones with rare dolomite grains	Calcisphaerae	Campanian	CAMPANIAN
B1b	Sutivan-Borak	Early dolomitized wackestones	Recrystallized rotaliids, small miliolids *Valvulina* aff. *triangularis* d'Orbigny, undeterminable rotaliids and miliolids		MAASTRICHTIAN? PALEOCENE?[3]
B1c	Sutivan-Borak	Wackestones	Discorbid-type of foraminifera, *Laginophora* sp., *Porochara* sp. (Charophyta), *Valvulina* sp.		PALEOCENE (THANETIAN?)
B1d	Sutivan-Borak	Wackestones	Ostracods, undeterminable rotaliids (some of them are dicorbid-type)		PALEOCENE (THANETIAN?)
B1e	Sutivan-Borak	Wackestones	Undeterminable rotaliids, *Valvulina* aff. *triangularis* d'Orbigny, ostracods		MAASTRICHTIAN? PALEOCENE?[3]
B1a	Sutivan-Borak	Wackestones	*Scandonea* sp., *Textularia* sp., *Fleuryana* sp., *Accordiella* sp.,		CAMPANIAN -

			fragments of echinoids, ostracods, undeterminable rotaliids and miliolids		MAASTRICHTIAN
B2	Postire	Dolomitized laminated microbial bindstones	Rare fragments of rotaliids and undeterminable numebucullariid forms		
B3	Mirca	Laminated mudstones Recrystallized mudstones			
B4	Sumartin	Dolomitized mudstones – wackestones	Fragments of bivalves, *Cuneolina* sp.		CRETACEOUS
B5	Splitska	Dolomitized mudstones – wackestones			
B8	Pučišča	Laminated microbial bindstones Dolomitized mudstones – wackestones	Undeterminable miliolids Undeterminable fragments of stomatoporids		
M14	Sutmiholjska bay	Oncoidal mudstones with cyanobacterial sheets, bindstones	*Clypeina jurassica* Favre, *Kurnubia* sp.	Late Jurassic	TITHONIAN
M8	Vrata Solina	Mudstones		Late Jurassic	LATE TITHONIAN – EARLY VALANGIAN
M11	Punta Križa	Dolomitized mudstones		Late Jurassic	LATE TITHONIAN – EARLY VALANGIAN
M6	Saplunara	Packstones with intraclasts and peloidal grains	Fragments of bivalves	Barremian - Albian	LATE HAUTREVIAN – EARLY BARREMIAN
M3	Okuklja bay	Mudstones with peloidal and cryptoalgal grains		Albian	EARLY BARREMIAN
M7	Paselo	Laminated wackestones, early diagenetic dolomites	*Nummuloculina* (*Pseudonummuloculina*) *heimi* Bonet, *Sabaudia* sp., *Nezzazata* sp., undeterminable miliolids	Late Cretaceous	LATE ALBIAN – MIDDLE CENOMANIAN
M1	Maranovići	Mudstones alternating with mudstones with scattered peloidal grains		Albian	ALBIAN
M5	Blato	Wackestones	*Cuneolina* sp., *Nummuloculina* (*Pseudonummuloculina*) sp., ostracods, fragments of bivalves	Albian	ALBIAN
M13	Lokve bay HR 1788-797	Laminated peloidal grainstones to peloidal wackestones	*Cuneolina pavonia parva* Henson, S*abaudia* sp., *Salpingoporella* sp., *Nummuloculina* (*Pseudonummuloculina*) sp., undeterminable miliolids	Albian	ALBIAN
M9	Sobra HR 1652-663	Packstones to grainstones		Late Cretaceous	ALBIAN? CENOMANIAN?

M12	Kozarica, HR 1758-767; 1813-828	Peloid-miliolid grainstones	*Nummuloculina regularis* Philippson, undeterminable miliolids	Barremian - Albian	CENOMANIAN
M10	Pomena 1+2, HR 1664-679, 1680-684	Packstones to grainstones, with peloidal grains	Undeterminable miliolids	Albian	CENOMANIAN
M4	Požura 1, HR 1580-589	Packstones to grainstones with peloidal grains	*Spiroloculina* sp., *Nummuloculina* (*Pseudonummuloculina*) sp.	Albian	CENOMANIAN
K1	Samograd bay	Laminated packstones (biomicrites)	*Thaumatoporella parvovesiculifera* (Ranieri), *Moncharmontia apenninica* (De Castro), *Cuneolina* sp., *Rotalia* sp., *Bolivinopsis* sp.	Coniacian – Maastrichtian	CONIACIAN - SANTONIAN
K2	Prižba	Well sorted grainstones (intrabiosparites)	*Bolivinopsis* sp., *Glomospira* sp., *Salpingoporella muehlberger* (Lorenz), *Debarina hahounerensis* Foucarde, Raoult & Vila	Barremian – Albian	LOWER APTIAN
K6	Karbuni	Wackestones, partly recrystalized	*Valdanchella decourti*" Decrouez & Moullarde, *Salpingoporella ? turgida* Radoičić, Bacinella-like forms, *Nummuloculina* (*Pseudonumuloculina*) sp.	Barremian – Albian	ALBIAN
K9	Blaca	Mudstones to laminated mudstones with scattered calcite crystals Alternation of micritic laminae with rare cyanobacterial filaments and cryptalgal laminae with cyanobacteral mats	*Thaumatoporella parvovesiculifera* (Ranieri), *Decastronema kotori* (Radoičić)	Turonian	TURONIAN
K5	Grščica	Mudstones to wackestones Laminated ostracod wackestones interbedded with grainstones	Ostracods, undeterminable miliolids *Thaumatoporella parvovesiculifera* (Raineri)	Barremian - Albian	BARREMIAN - ALBIAN
K3	Karbuni - 2	Laminated biomicrobial mudstones (bindstones)	Bacinella-like forms, *Thaumatoporella parvovesiculifera* (Raineri), undeterminable agglutinated small benthic (*Mayncina* sp.?, *Novalesia* sp.?) foraminifera and rotaliids, rare undeterminable miliolids, fragments of bivalves, ostracods	Barremian - Albian	ALBIAN
K7	Gornja Potira	Grainstones, well sorted (biosparites)	Fragments of *Chondrodonta* shells, *Cuneolina pavonia* d'Orbigny, *Nezzazatinell*a sp., *Chrysalidina* sp.,	Cenomanian - Turonian	CENOMANIAN

			Pastrikella (*Broeckina*) sp., *Nummuloculina* (*Pseudonummuloculina*) sp., undeterminable miliolids		
K8	Zavalatica	Laminated recrystallized biomicrobial mudstones (micrites)	*Thaumatoporella parvovesculifera* (Raineri), undeterminable rotaliids	Cenomanian - Turonian	CENOMANIAN - TURONIAN
K4	Blaca – 2	Laminated mudstones, alternation of micritic laminae with rare cyanobacterial filaments and cryptalgal laminae with cyanobacteral mats	*Thaumatoporella parvovesculifera* (Raineri), ostracods, undeterminable miliolids, *Decastronema kotori* (Radoičić)	Turonian	TURONIAN
K10	Babina	Grainstones	Undeterminable miliolids, fragments of gastropods, *Thaumatoporella parvovesiculifera* (Raineri), *Nummuloculina* (*Pseudonummuloculina*) *heime* Bonet	Lower Cretaceous (Barremian - Albian)	ALBIAN
K11	Babina Smokvica	Mudstones with a lot of sparite infilled cracks	*Thaumatoporella parvovesiculifera* (Raineri), undeterminable rotaliids (*Epistomaria* sp.?) and miliolids, fragments of rudist shells	Coniacian – Maastrichtian	CONIACIAN – MAASTRICHTIAN
H1	Perna bay	Bindstones, changes in density of micrites		Senonian	CAMPANIAN
H2	Zaglav	Packstones	Fragments of rudist shells, undeterminable miliolids	Coniacian-Campanian	SANTONIAN
H3	Poljica - Stiniva	Wackestones	Undeterminable miliolids *Chrysalidina* sp.	Senonian	CENOMANIAN
H4	Poljica – Stiniva (close to the road)	Packstones - grainstones	*Chrysalidina* sp., *Scandonea* sp. undeterminable miliolids, fragments of bivalves	Senonian	TURONIAN CENOMANIAN
H5	Nova crkva	Wackestones	*Thaumatoporella parvovesiculifera* (Raineri), *Chrysalidina* sp., *Scandonea* sp.	Turonian	CENOMANIAN? TURONIAN-SANTONIAN
H6	Lozna bay	Early diagenetic dolomites, patches of original sediments: micrite matrix around microfossils	*Dicyclina* sp., undeterminable miliolids, *Decastronem*a sp. *Moncharmontia apenninica* (De Castro), *Thaumatoporella parvovesiculifera* (Raineri), *Scandonea* sp.	Coniacian - Campanian	TURONIAN - SANTONIAN
H7	Maslinica bay	Wackestones to mudstones			CENOMANIAN
H8	Stiniva bay	Wackestones	*Nummuloculina* (*Pseudonummuloculina*) *heimi* Bonet, *Thaumatoporella parvovesiculifera* (Raineri), *Decastronema kotori* (Radoičić)	Coniacian - Campanian	TURONIAN SANTONIAN (CENOMANIAN - CAMPANIAN)
H9	Vira bay	Wackestones	*Scandonea sammitica* De Castro,	Coniacian -	TURONIAN -

			Moncharmontia apenninica (De Castro), *Thaumatoporella parvovesiculifera* (Raineri)	Campanian	SANTONIAN
H10	Vira II	Wackestones	*Scandonea sammitica* De Castro, *Moncharmontia apenninica* (De Castro), *Thaumatoporella parvovesiculifera* (Raineri)	Coniacian - Campanian	TURONIAN - SANTONIAN
H11	Gromin dolac	Laminated wackestones to mudstones	*Thaumatoporella parvovesiculifera* (Raineri), *Decastronema kotori* (Radoičić)	Coniacian - Campanian	TURONIAN - SANTONIAN
H12	Soča bay	Laminated wackestones	*Accordiella conica* Farinacci, *Dicyclin*a sp. *Moncharmontia apenninica* (De Castro), *Rotalispira scarsellai* (Torre), *Decastronema kotori* (Radoičić)	Coniacian - Campanian	TURONIAN - SANTONIAN
H13	Križišće - Poljica	Partly washed micritic limestones (bimicrites), laminated pelletal wackestones to mudstones	*Thaumatoporella parvovesiculifera* (Raineri), *Decastronema kotori* (Radoičić), undeterminable miliolids, *Pastrikella balcanica* (Cherchi, Radoičić & Schroeder)	Cenomanian - Turonian	CENOMANIAN
H14	Rudine	Laminated pelletal wackestones and packstones	*Moncharmontia apenninica* (De Castro)	Cenomanian - Turonian	TURONIAN - SANTONIAN
H15	Basina	Laminated packstones to wackestones	*Nezzazata* sp., *Thaumatoporella parvovesiculifera* (Raineri), *Pastrikella* (*Broeckina*) *balcanica* (Cherchi, Radoičić & Schroeder)	Cenomanian - Turonian	CENOMANIAN
H16	Zavala bay	Packstones	*Thaumatoporella parvovesiculifera* (Raineri), *Decastronema kotori* (Radoičić), fragments of gastropods, bivalves	Cenomanian - Turonian	TURONIAN - SANTONIAN
H17	Bristova	Contact between packstones and wackestones	*Thaumatoporella parvovesiculifera* (Raineri), undeterminable miliolids, *Murgella* sp.	Turonian	TURONIAN - SANTONIAN
H19	Pitve	Wackestones	Fragments of bivalves	Lower Cretaceous	NEOCOMIAN
H18	Jelsa	Mudstones		Lower Cretaceous	BARREMIAN OR LATE APTIAN - EARLY ALBIAN

(*) Oštrić, N., Jelaska, V., Fuček, L., Prtoljan, B., Korolija, B., Gušić, I., Marinčić, S., Šparica, M., Korbar, T., Husinec, A., 2015, Basic geological map of the Republic of Croatia, Sheet Island of Hvar 1. 50 000, Zagreb, Croatian Geological Survey
(**) Geological Map of the Republic of Croatia at the Scale 1: 300 000, 2010
after: (1) Schlagintweit et al., 2017; (2) Consorti et al., 2017;. And (3) Granero et al., 2019

Supplementary Table 2. List of the localities providing no paleomagnetic result, mainly due to extremely weak NRM.

		Locality	Age	Lat (˚) Lon (˚)	Dip
		Brač			
1	B18	Zagvozd HR2223-228	Cenomanian - Coniacian	43°17'58" 16°46'39"	31/8, 28/10
2	B9	Grašišče HR2305-315	Upper Turonian - Lower Campanian	43°17'18" 16°42'34"	32/19
3	B9	Grašišče HR2452-470	Upper Turonian - Lower Campanian	43°17'19" 16°42'34"	20/9
4	B8	Pučišča HR2276-281	Upper Turonian - Lower Campanian	43°21'31" 16°44'31"	20/21
5	B8	Pučišča HR2336-349	Upper Turonian - Lower Campanian	43°21'31" 16°44'31"	5/21
6	B14	Milna, olive grove HR2410-422	Coniacian - Campanian	43°19'02" 16°26'50"	197/22
7	B13	Grižev promontory HR2363-375	Campanian	43°17'22" 16°29'23"	180/19
8	B7	Pučišča, road cut HR2442-451	Campanian	43°21'14" 16°44'27"	13/22
9	B1f	Sutivan HR2400-409	Thanetian (Paleocene)	43°23'20" 16°27'36"	23/15
10	B1g	Sutivan HR2259-263	Ypresian	43°23'26" 16°27'05"	335/23
11	B1h	Sutivan HR2264-275	Ypresian	43°23'26" 16°27'05"	5/25
		Mljet			
12	M6	Saplunara HR1622-629, 1685-698	Upper Hauterivian - Lower Barremian	42°42'31" 17°43'35"	26/14
13	M5	Blato HR1612-621	Albian	42°46'13" 17°27'58"	353/54
14	M9	Sobra HR1652-663	Albian - Cenomanian?	42°44'46" 17°35'60"	21/39
15	M2	Požura HR1580-589	Cenomanian	42°43'42" 17°39'02"	12/38

Supplementary Table 2, 2/3

		Locality	Age	Lat (˚) Lon (˚)	Dip
16	M4	Požura HR1602-611	Cenomanian	42°43'42" 17°38'42"	11/34
17	M10	Pomena HR1664-684	Cenomanian	42°46'51" 17°19'50"	229/62, 234/54, 348/25
		Korčula			
18	K2	Prižba HR1778-787	Lower Aptian	42°54'25" 16°47'22"	179/50
19	K3	Karbuni-2 HR1977-984	Albian	42°55'17" 16°43'42"	196/65, 200/61
20	M7	Gornja Potira HR1985-998	Cenomanian	42°56'03" 16°42'50"	191/51
21	K11	Babina Smokva HR2031-040	Coniacian - Maastrichtian	42°58'25" 16°57'31"	333/24
		Hvar			
22	H18	Jelsa HR2216-222	Barremian - Albian	43°09'18" 16°40'39"	74/16
23	H6	Lozna bay HR2069-078	Turonian - Santonian	43°13'23" 16°31'33"	340/27
24	H8	Busje, Stiniva bay HR2095-105	Turonian - Santonian	43°12'06" 16°28'04"	347/30
25	H2	Zaglav HR1944-951	Santonian	43°07'04" 17°03'02"	170/45
		Vis			
26	V5	Kupinovac HR896-901	Albian	43°00'06" 16°05'22"	179/44
27	V6	Stupišče HR887-895	Cenomanian	43°00'25" 16°04'20"	138/39
28	V10	Dragodir HR1551-561	Cenomanian	43°03'39" 16°05'02"	353/43, 346/46
29	V8	Vis Town, Bandirica HR1539-544	Cenomanian	43°03'45" 16°10'55"	70/11
30	V14	Promontory Parja HR1512-523	Turonian – Lower Santonian	43°04'41" 16°11'05"	358/24

Supplementary Table 2, 3/3

		Locality	Age	Lat (˚) Lon (˚)	Dip
31	V15	Uvala Tiha HR911-916	Turonian – Lower Santonian	43°04'25" 16°07'38"	9/52
32	V17	Oključna HR902-910	Turonian – Lower Santonian	43°04'26" 16°07'22"	6/32
33	V24	Mala Travna Uvala HR927-938	Turonian – Lower Santonian	43°01'12" 16°10'45"	156/18